

Supporting Information

Glycosylated AIE-active Fe (III) photosensitizer activated by tumor microenvironment for synergistic type I photodynamic and chemodynamic therapy

Gai-Li Feng, Wei Zhou, Jin-pin Qiao, Guang-Jian Liu, and Guo-Wen Xing

College of Chemistry, Beijing Normal University, Beijing 100875, P. R. China.

Table of Contents

Table of Contents	1
1. General information	2
2. Synthesis of BT-TPE and BT-TPE@Fe-Lac	7
3. Supporting tables and figures.....	12
4. NMR spectra and MS spectra	25

1. General information

1.1 Materials and Instruments

Materials and reagents were purchased from commercial suppliers and used without further purification. All solvents were analytical pure unless otherwise noted. Distilled water was used throughout the experiments. TLC analysis was used to monitor the course of reaction on silica gel plates (HSGF254) and column chromatography was carried on with silica gel (mesh 200-300). Absorption spectra of liquid samples were determined on Hitachi UV-3900 spectrophotometer. The fluorescence spectra were recorded by an Edinburgh Instruments FS5 fluorescence spectrometer. Fourier Transform Infrared (FTIR) Spectra were recorded on an IRAffinity-1 spectrometer. Transmission electron microscope (TEM) images were obtained using a FEI Talos F200S instrument. NMR spectra were recorded with JEOL-400 or JEOL-600 spectrometers. Dynamic Light Scattering (DLS) were performed on Zeta Potential Analyzer (Brookhaven Instruments Corporation, America). Confocal fluorescence imaging was performed with Nikon A1R MP multiphoton microscopy. Cell viability test was obtained on a Thermo Scientific Multiskan. Irradiation was performed using a High power LED lamp source (white light: 400-800nm, PLS-LED 100C, Beijing Perfectlight Technology Co., Ltd, Beijing, China). Flow cytometry test of apoptosis were carried out with a CytoFLEX (BECKMAN) instrument.

1.2 FTIR Spectra.

The dry power sample of **BT-TPE@Fe-Lac/Fe-Lac** is pressed into anhydrous KBr particles and analyzed on an IRAffinity-1 spectrometer.

1.3 Determination of Fe²⁺ generation.

Preparation of test sample solution: Take **BT-TPE@Fe-Lac**(2mM) 100uL and then add 100uL of GSH (1mM).

Standard curve drawing: Add different volumes of Fe²⁺ solution (0.01mM) to 1mL

1,10-Phenanthroline (0.5 mM), then add PBS to make the volume of the test solution 2mL, and test the absorption changes through UV absorption spectroscopy.

Work Curve drawing: Add different volumes of test samples to 1mL 1,10-Phenanthroline solution (0.5 mM) and 1 mL GSH solution (1mM), the generation of Fe²⁺ was measured by UV/VIS absorption spectroscopy, and the characteristic absorption band of the Fe (II) phenanthroline complex at 512 nm was strongly augmented with

increasing concentrations of GSH.

1.4 Oxidation detection of GSH

Preparation of test sample solution: Take **BT-TPE@Fe-Lac** (2mM) 100uL and then add 100uL of GSH (1mM).

Standard curve drawing: Add different volumes of GSH solution (1mM) to 1mL DTNB (1mM), then add PBS to make the volume of the test solution 2mL, and test the absorption changes through UV absorption spectroscopy.

Work Curve drawing: Add different volumes of test samples to 1mL DTNB (1mM) and 1mL GSH (1mM) solution, the consumption of GSH was measured by UV/VIS absorption spectroscopy, and the decrease in absorption at 412nm indicates the consumption of GSH.

1.5 Detection of $\cdot\text{OH}$ production with ABTS in solution

We employed 2,2'-azino-bis (3-ethylbenzothiazoline-6-sulfonic acid) (ABTS)(1mM) as a specific $\cdot\text{OH}$ probe to detect the generation of $\cdot\text{OH}$ in solution. When $\cdot\text{OH}$ is generated in the system, ABTS can be oxidized and the absorption at 416, 648, 732 and 818 nm increase.

Preparation of test sample solution: i) 10 μM of **BT-TPE@Fe-Lac** was dispersed in water containing 1mM of ABTS; ii) 10 μM of **BT-TPE@Fe-Lac** or **BT-TPE** was dispersed in water containing ABTS (1mM) and GSH (1mM); iii) 10 μM of **BT-TPE@Fe-Lac** or **BT-TPE** was dispersed in water containing ABTS(1mM), GSH (1mM) and H_2O_2 (1mM); iv) GSH (2mM) was dispersed in water containing of ABTS (1mM), H_2O_2 (1mM) and GSH (2mM).

1.6 Detection of $\text{O}_2^{\cdot-}$ production in solution

We employed dihydroethidium (DHE) as a specific $\text{O}_2^{\cdot-}$ probe to detect the generation of $\text{O}_2^{\cdot-}$ in solution. When $\text{O}_2^{\cdot-}$ is generated in the system, DHE can be oxidized to form ethidium which intercalates into DNA and emits bright fluorescence at ~ 580 nm. Specifically, 10 μM of **BT-TPE@Fe-Lac** was dispersed in 2 mL PBS containing 40 μM of DHE and 500 $\mu\text{g/mL}$ ctDNA. The mixture was then placed in a cuvette and irradiated with a 400-800 nm LED light at 40 mW/cm^2 . The fluorescence of the sample at 580 nm was recorded by the Hitachi F-4600 spectrophotometer.

1.7 $\text{O}_2^{\cdot-}$ detection by ESR spectroscopy

Electron spin resonance (ESR) spectroscopy was employed to detect the generation of $\text{O}_2^{\cdot-}$. DMPO (5-tert-

butoxycarbonyl 5-methyl-1-pyrroline N-oxide) was used as a spin-trap agent for $O_2^{\cdot-}$. ESR spectroscopy was employed to detect the ESR signals of the following five groups of samples: i) 120 μ M of **BT-TPE** was dispersed in water containing 25 mM of DMPO illuminated with a xenon lamp (500-1200 nm); ii) 120 μ M of **BT-TPE** were dispersed in water containing 25 mM of DMPO without light-irradiation; iii) 120 μ M of **BT-TPE@Fe-Lac** was dispersed in water (pH=5.4) containing 25 mM of DMPO illuminated with a xenon lamp (500-1200 nm); iv) 120 μ M of **BT-TPE@Fe-Lac** was dispersed in water (pH=5.4) containing 25 mM of DMPO illuminated without light-irradiation. v) 120 μ M of **BT-TPE@Fe-Lac** was dispersed in water (pH=7.4) containing 25 mM of DMPO illuminated with a xenon lamp (500-1200 nm); The ESR signals are recorded by the Bruker E500 instrument.

1.8 \cdot OH detection by ESR spectroscopy

Electron spin resonance (ESR) spectroscopy was employed to confirm the generation of \cdot OH. DMPO (5,5-Dimethyl-1-Pyrroline-N-Oxide) was used as a spin-trap agent for \cdot OH. ESR spectroscopy was employed to detect the ESR signals of the following four groups of samples: i) 120 μ M of **BT-TPE@Fe-Lac** or **BT-TPE** was dispersed in water containing 25 μ M of DMPO; ii) 120 μ M of **BT-TPE@Fe-Lac** or **BT-TPE** was dispersed in water containing 25 mM of DMPO and GSH (2mM); iii) 120 μ M of **BT-TPE@Fe-Lac** or **BT-TPE** was dispersed in water containing 25 mM of DMPO and H_2O_2 (2mM); iv) 120 μ M of **BT-TPE@Fe-Lac** or **BT-TPE** was dispersed in water containing 25 mM of DMPO, H_2O_2 (2mM) and GSH (2mM). The ESR signals are recorded by the Bruker E500 instrument.

1.9 In vitro cytotoxicity

The HepG2 cells were seeded in a 96-well plate with culture media. After 24 h, 1 μ M of **BT-TPE@Fe-Lac** were incubated with cells for 10 h. Then, the cells were washed three times with PBS, and infused with fresh medium. After further incubation for different times, and illuminated by a LED light (400-800 nm, 40 mW / cm^2) for 20 min. Cells were allowed to continue growing for 24 h. Then, 10 μ L MTT solutions (5 mg/mL) in PBS were added to each well. The produced formazan was dissolved in 0.1 ml of dimethylsulfoxide (DMSO) and the absorbance was measured using a microplate reader (Biotek Epoch). Cell viability was expressed as a percentage of the control culture value. Moreover, the dark toxicity of **BT-TPE@Fe-Lac** was also analyzed by the above procedure except the illumination was eliminated.

1.10 ROS generation in living cells

In vitro catalytic ROS generation was evaluated by employing 2,7-Dichlorodihydrofluorescein diacetate (DCFH-DA) as the fluorescent indicator. HepG2 cells were planted onto 35-mm confocal dishes at a density of 1×10^5 cells. After incubation for 24 h under normoxic (21% O₂) or hypoxic (2% O₂) conditions, the medium was removed and washed with PBS three times. Then, HepG2 cells were incubated with 1 μ M **BT-TPE@Fe-Lac** for different times and then washed with PBS three times. Then, the cells were incubated with the fluorescent probe DCFH-DA (20 μ M) for 30 min at 37 °C in the dark and then were washed three times with PBS. The cells were subsequently treated with LED irradiation (400-800 nm, 40 mW/ cm²) for 20 min and were successively examined by the CLSM.

1.11 Live/dead cell staining assay

The HepG2 cells were planted onto 35-mm confocal dishes at a density of 1×10^5 cells. After 24 h, 1 μ M of **BT-TPE@Fe-Lac** or **BT-TPE** was incubated with cells for different time. The cells were washed with PBS three times. After exposure to a LED light (400-800 nm, 40 mW/ cm²) for 20 min, the cells were cultured for another 24 h and then stained with calcein acetoxymethyl ester (calcein AM) and propidium iodide (PI) for 30 min. Fluorescent images were promptly captured by Nikon single-particle microscopy with a 20 \times objective lens. Moreover, the dark toxicity of **BT-TPE@Fe-Lac** was also analyzed by the above procedure except the illumination was eliminated.

1.12 Flow Cytometry Test of Apoptosis.

The HepG2 cells were cultured in 6-well plates, and treated with **BT-TPE@Fe-Lac** (2 μ M) or **BT-TPE** (2 μ M). Then, the cells were irradiated with a LED light (400-800 nm, 40 mW/cm²) for 20 min. After further incubation for 24 h, the cells were collected and treated with AnnexinV-FITC/PI cell apoptosis detection kit. The flow cytometry was used to detect cell apoptosis.

1.13 Intracellular GSH depletion

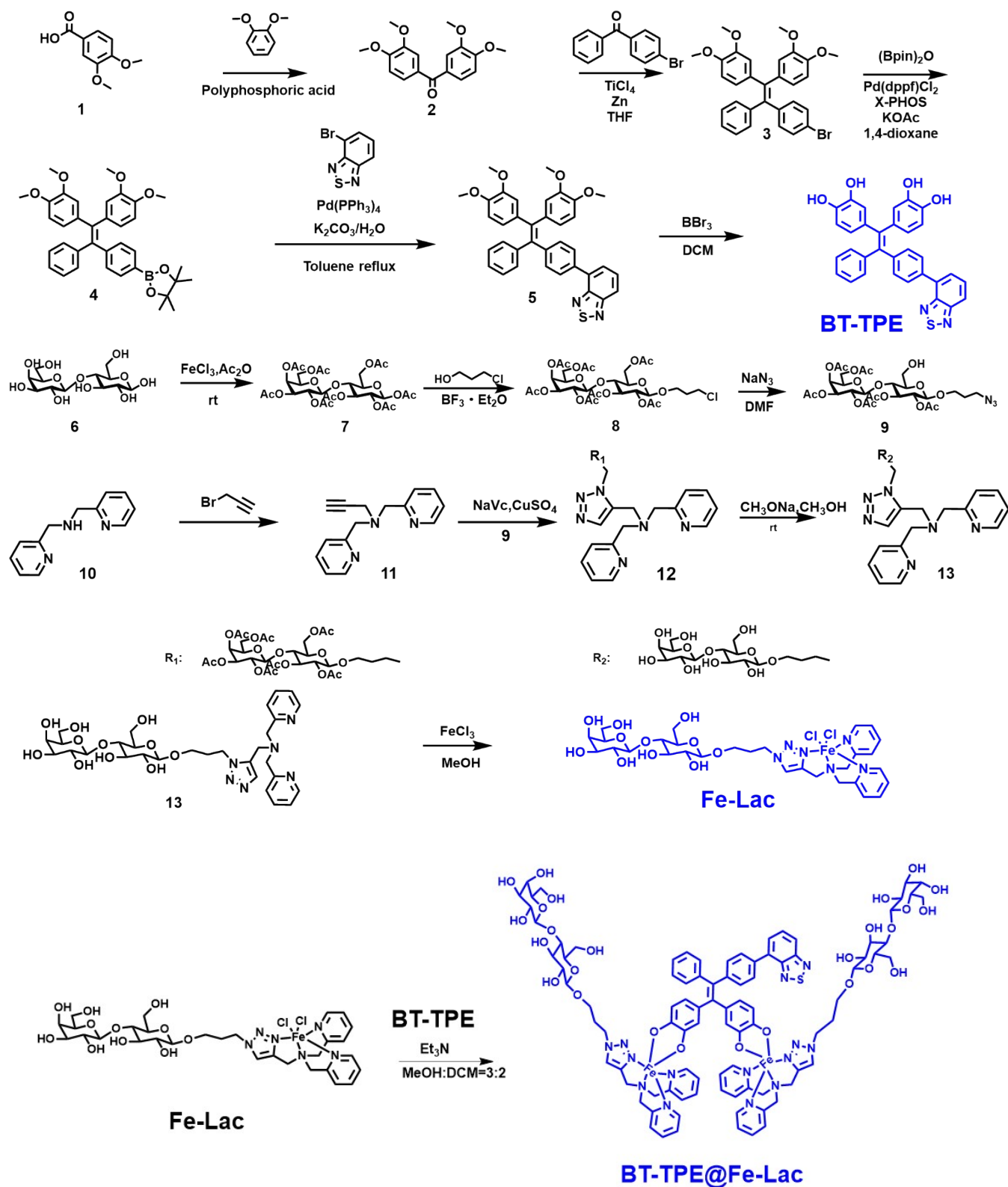
The HepG2 cells were seeded into 6-well plate and treated with PBS, **BT-TPE** (100 μ M), and **BT-TPE@Fe-Lac** (100 μ M) cultivated for 24 h, respectively. Next, after digested, resuspended and fragmented, they were then centrifuged at 10000 rpm for 10 min and the supernatants collected. The GSH level of each group was tested by a Reduced Glutathione (GSH) Content Assay Kit through UV/VIS absorption spectroscopy.

1.14 Test of Cell death mode

The HepG2 cells were plated in 96-well plates at a density of 5,000 cells per well and allowed to incubate for a

duration of 24 hours. Subsequent to this incubation, the culture medium was replaced with DMEM containing various ingredients in different wells: i) **BT-TPE@Fe-Lac** (0 μM) or **BT-TPE** (0 μM); ii) **BT-TPE@Fe-Lac** (0.5 μM) / **BT-TPE** (0.5 μM) and Ferrostatin-1 (20 μM); iii) **BT-TPE@Fe-Lac** (0.5 μM) / **BT-TPE** (0.5 μM) and Z-VAD-FMK (20 μM); iv) **BT-TPE@Fe-Lac** (0.5 μM) / **BT-TPE** (0.5 μM) and 3-methyladenine (20 μM); v) **BT-TPE@Fe-Lac** (0.5 μM) / **BT-TPE** (0.5 μM) and Necrostatin (20 μM). Following this, the plate was allowed to further incubate for an additional 3 hours. Subsequently, the cells in the plate were subjected to light irradiation at a wavelength of 400-800 nm and an intensity of 40 mW/cm² for a duration of 20 minutes. After the irradiation, the cells were again incubated for an additional 24 hours. The viability of the cells was assessed using a MTT assay, following the proposed protocol. The results of the cell viability measurements were obtained using Thermo Scientific Multiskan reader.

2. Synthesis of BT-TPE and BT-TPE@Fe-Lac.



Scheme S1. Synthetic route for BT-TPE@Fe-Lac.

Synthesis of Compound 2: 2 g (10.98 mmol) of 3,4-dimethoxybenzoic acid **1** and 1.52 g (10.98 mmol) of 1,2-dimethoxybenzene were stirred in 20 g of polyphosphoric acid at 80 °C for 1 h. The mixture was then cooled to 60 °C, and 250 mL of water was added over 30 min. The precipitate was filtered and dissolved in 100 mL CH₂Cl₂, washed with brine water successively. The organic phase was dried over anhydrous Na₂SO₄ and concentrated in vacuo. Recrystallization with methanol to give 3 g **2**, yield 90.39 %.

¹H NMR (600 MHz, Chloroform-*d*) δ 7.40 (d, *J* = 1.6 Hz, 2H), 7.35 (dd, *J* = 8.3, 1.7 Hz, 2H), 6.88 (s, 2H), 3.92 (d, *J* = 12.4 Hz, 13H).

Synthesis of Compound 3: Add compound **2** (3,3,4,4-tetramethoxy benzophenone, 1g, 3.3 mmol), 4-bromodibenzophenone, 0.86 g, (3.3 mmol), Zn powder (1.51 g, 23.1 mmol), and magnetic particles to flasks with three neck in sequence, connect the reflux tube, seal the system, and exchange nitrogen gas three times. Add 22 mL of anhydrous tetrahydrofuran (THF) solvent, cool the entire system at -70 °C for 10 minutes, and then add TiCl₄ (1.37mL, 9.9mmol) dropwise. Then, stir the reaction system until it reaches room temperature, where the reaction solution turns black. Then, place it in an oil bath and heat it up to 70 °C, reflux and stir overnight. After the reaction is completed, stop heating the reaction and cool it to room temperature. Quench the reaction thoroughly with 10 mL of 10% K₂CO₃ aqueous solution and stir for about 2 hours. Filter with diatomaceous earth to obtain a yellow solution. The filtrate was washed with saturated sodium bicarbonate and saturated sodium chloride, extracted with dichloromethane, and the organic phase was collected and dried with anhydrous sodium sulfate for about half an hour. The sodium sulfate was filtered out and the solvent was removed using a rotary evaporator. The crude product was separated by silica gel column chromatography (pure petroleum ether separation), and the TLC developing agent was petroleum ether: ethyl acetate=5:1, resulting in a pale yellow solid compound **3**, yield 33.3%.

¹H NMR (600 MHz, Chloroform-*d*) δ 7.22 (d, *J* = 8.4 Hz, 2H), 7.10 (dt, *J* = 13.8, 6.9 Hz, 3H), 7.02 – 6.99 (m, 2H), 6.89 (d, *J* = 8.4 Hz, 2H), 6.64 (d, *J* = 8.3 Hz, 1H), 6.62 (d, *J* = 8.3 Hz, 1H), 6.59 – 6.54 (m, 2H), 6.52 (d, *J* = 5.4 Hz, 2H), 3.83 (s, 3H), 3.81 (s, 3H), 3.54 (s, 3H), 3.46 (s, 3H).

¹³C NMR (150 MHz, CHLOROFORM-*D*) δ 148.06, 147.95, 147.88, 147.84, 143.94, 143.44, 141.22, 138.10, 135.84, 135.81, 132.95, 131.62, 131.25, 131.01, 128.73, 128.30, 128.15, 128.03, 127.88, 126.61, 126.56, 126.50, 126.24, 125.91, 124.29, 124.18, 120.19, 115.16, 115.09, 110.44, 110.27, 56.01, 55.78, 55.74, 55.69, 55.64, 55.59.

HRMS (ESI): *m/z* calcd for [C₃₀H₂₇BrNaO₄]: 553.0984; Found: 553.0978.

Synthesis of Compound 4: Anhydrous and anaerobic reactions are carried out in an infrared light box drying

experiment using two bottles, reflux tubes, reverse stoppers, magnets, and syringes. Water removal operations are carried out using 4 Å molecular sieves. Afterwards, compound 3 (0.25g,0.41mmol), bis(pinacolato)diboron (104.1mg, 0.41mmol), Pd₂(dba)₃(18.8mg, 0.0205mmol), X-PHOS (39.1mg, 0.082mmol), KOAc (201.2mg, 2.05mmol), and magnetic particles were sequentially added to the reaction flask. The system was sealed and replaced with nitrogen gas three times. Add 10mL of solvent dioxane and reflux at 88 °C for more than 4 hours. After the reaction is completed, the system is cooled and filtered to remove the Pd catalyst precipitate. The solvent is washed with DCM and removed using a rotary evaporator. The crude product was separated by silica gel column chromatography (petroleum ether/ethyl acetate=20/1), and the TLC developing agent was petroleum ether: ethyl acetate=5:1 to obtain a yellow solid **compound 4**, yield 80.72 %.

¹H NMR (600 MHz, Chloroform-*d*) δ 7.55 (d, *J* = 7.4 Hz, 2H), 7.10 (d, *J* = 7.5 Hz, 2H), 7.03 (dd, *J* = 18.5, 7.7 Hz, 4H), 6.64 (d, *J* = 8.3 Hz, 2H), 6.59 (d, *J* = 4.6 Hz, 2H), 6.54 (s, 2H), 3.83 (s, 6H), 3.47 (s, 6H), 1.32 (s, 12H).

¹³C NMR (150 MHz, CHLOROFORM-*D*) δ 147.86, 147.78, 147.74, 147.59, 144.24, 141.03, 139.35, 136.10, 136.05, 135.07, 134.33, 131.28, 131.25, 130.99, 130.63, 128.97, 128.59, 127.89, 127.69, 126.30, 126.24, 125.84, 124.44, 124.21, 124.20, 123.55, 115.34, 115.28, 114.15, 110.27, 110.24, 83.86, 75.15, 55.90, 55.74, 55.71, 55.67, 55.63, 29.78, 24.93, 24.65.

HRMS (ESI): *m/z* calcd for[C₃₆H₃₉BO₆Na]: 601.2738; Found: 601.2746.

Synthesis of Compound 5: Anaerobic reaction, compound 4 (50mg, 0.086mmol), 4-bromo-2,1,3-benzothiadiazole (18.59 mg, 0.086mmol), Pd (PPh₃)₄ (9.9 mg, 0.0086 mmol), and magnetic particles were sequentially placed in two 25 mL bottles. The system was sealed, and nitrogen gas was exchanged three times. Then, 5mL of toluene was injected. K₂CO₃ (47.54 mg, 0.344 mmol) was dissolved in 0.5 mL H₂O and added to the reaction system by injection. The reaction system was heated at 80 °C and refluxed overnight until the end of the reaction. Cool the reaction mixture to room temperature. Remove solvent by rotary evaporation. Pour the residue into water and extract with DCM. Dry the organic layer with MgSO₄, filter and remove the solvent by rotary evaporation. The crude product was separated by silica gel column chromatography (petroleum ether: ethyl acetate=20:1), and the TLC developing agent was petroleum ether: ethyl acetate=5:2 to obtain the compound 5, yield 88.74 %.

¹H NMR (600 MHz, Methanol-*d*₄) δ 7.92 (d, *J* = 8.6 Hz, 1H), 7.73 (d, *J* = 8.2 Hz, 2H), 7.71 (d, *J* = 7.1 Hz, 1H), 7.68 (d, *J* = 7.0 Hz, 1H), 7.13 – 7.08 (m, 4H), 7.07 – 7.02 (m, 3H), 6.54 (d, *J* = 1.9 Hz, 1H), 6.51 (dd, *J* = 8.1, 1.4 Hz, 1H), 6.47 (d, *J* = 2.0 Hz, 1H), 6.47 – 6.45 (m, 1H), 6.41 (dd, *J* = 8.1, 2.0 Hz, 1H), 6.34 (dd, *J* = 8.1, 2.0 Hz, 1H).

¹³C NMR (150 MHz, CHLOROFORM-*D*) δ 155.74, 153.47, 147.99, 147.89, 147.79, 144.66, 144.27, 141.11, 138.95,

136.13, 136.09, 135.14, 134.25, 131.49, 131.39, 129.69, 128.71, 127.99, 127.48, 126.39, 124.33, 124.28, 120.42, 115.42, 115.35, 110.37, 110.26, 77.34, 77.13, 76.91, 55.78, 55.76, 55.67, 29.78.

HRMS (ESI): m/z calcd for $[C_{36}H_{30}N_2O_4NaS]$: 609.1818; Found:609.1813.

Synthesis of Compound **BT-TPE**: Weigh compound 5 (0.05 g, 0.085 mmol) in a round bottom flask, seal the reaction system, and replace the gas in the system with high-purity nitrogen three times. Add 10 mL of anhydrous CH_2Cl_2 , stir the reaction system in an ice bath for 10 minutes, and then add BBr_3 (8.5 mL, 8.5 mmol) dropwise to the reaction system. Continue stirring in the ice bath for 10 minutes and stir overnight at room temperature. After TLC monitoring confirms that the reaction is complete, add water to quench the reaction. Extract with CH_2Cl_2 , wash three times with saturated NaCl solution and $NaHCO_3$ solution, merge the organic phase, and dry with anhydrous $MgSO_4$ for half an hour. The solvent was removed by rotary evaporation for concentration, and the crude product was separated by silica gel column chromatography (TLC developing agent: PE/EtOAc=1:1) to obtain 0.03 g of yellow solid **BT-TPE** with a yield of 66.34%.

1H NMR (600 MHz, Methanol- d_4) δ 7.92 (d, $J = 8.6$ Hz, 1H), 7.73 (d, $J = 8.2$ Hz, 2H), 7.71 (d, $J = 7.1$ Hz, 1H), 7.68 (d, $J = 7.0$ Hz, 1H), 7.13 – 7.08 (m, 4H), 7.07 – 7.02 (m, 3H), 6.54 (d, $J = 1.9$ Hz, 1H), 6.51 (dd, $J = 8.1, 1.4$ Hz, 1H), 6.47 (d, $J = 2.0$ Hz, 1H), 6.47 – 6.45 (m, 1H), 6.41 (dd, $J = 8.1, 2.0$ Hz, 1H), 6.34 (dd, $J = 8.1, 2.0$ Hz, 1H).

^{13}C NMR (151 MHz, DMSO- D_6) δ 170.84, 155.72, 153.14, 145.05, 144.91, 144.85, 144.69, 144.56, 142.19, 137.24, 135.43, 135.39, 134.61, 133.37, 132.16, 131.44, 131.35, 130.68, 129.22, 128.86, 128.30, 128.18, 126.51, 122.95, 122.93, 120.74, 118.81, 118.75, 115.52, 115.34.

HRMS (ESI): m/z calcd for $[C_{32}H_{23}N_2O_4S]$: 531.1373; Found:531.1374.

Synthesis of **Compound 7**: Ferric chloride (0.5 g, 3.1 mmol) was firstly dissolved in Acetic anhydride (30 mL, 318 mmol). Then, the lactose (5.0 g, 15 mmol) was added in batches to the reaction system and stirred at room temperature for 12 h. The mixture was extracted by EtOAc and washed by aqueous sodium hydrogen carbonate three times after stirring at ambient temperature for 4 h. Next, the mixture was to dry with anhydrous magnesium sulfate and remove the solvent by a rotary evaporator. Finally, the obtained solid was purified by column chromatography with Hex/ EtOAc (1:1, v/v). Yield: 9.12 g (92.0 %)

Synthesis of **Compound 8**: compound 7 (1.02 g, 2.00 mmol) was put into a 25 mL flask under argon protection. The 1-Chloro-3-hydroxypropane (0.36 g, 4.00 mmol) was dissolved in dry CH_2Cl_2 (8 ml), and the solution was added to the reaction. Adding $BF_3 \cdot Et_2O$ slowly at 0 °C (1.02 g, 7.20 mmol) and the reaction system was then stirred

at 36 °C for 8 h. After that, the reaction was washed with saturated salt water. The following process was to dry organic phase with anhydrous magnesium sulfate and remove the solvent by a rotary evaporator. Finally, the obtained solid was purified by column chromatography with Hex/EtOAc (1:2, v/v). Yield: 0.411 g (28.8 %).

¹H NMR (600 MHz, Chloroform-*d*) δ 5.34 (s, 1H), 5.19 (t, *J* = 9.3 Hz, 1H), 5.12 – 5.07 (m, 1H), 4.99 – 4.93 (m, 1H), 4.87 (t, *J* = 8.8 Hz, 1H), 4.51 – 4.41 (m, 3H), 4.15 – 4.05 (m, 3H), 3.94 (dt, *J* = 10.1, 5.2 Hz, 1H), 3.86 (t, *J* = 6.7 Hz, 1H), 3.78 (t, *J* = 9.5 Hz, 1H), 3.68 – 3.64 (m, 1H), 3.61 – 3.56 (m, 2H), 2.14 (s, 3H), 2.11 (s, 3H), 2.08 – 2.00 (m, 25H), 1.95 (s, 3H).

Synthesis of Compound 9: Compound 8 (0.357 g, 0.500 mmol) was added to a suspension of NaN₃ (65.0 mg, 1.00 mmol) in dry DMF (5 mL) at reflux for 16 h with stirring. The reaction mixture was concentrated in vacuo, and the residue was diluted with EtOAc. The organic layer was washed with H₂O and brine, dried over NaSO₄, filtered, and concentrated in vacuo. Yield: (0.351 g, 97.4%).

¹H NMR (600 MHz, Chloroform-*d*) δ 5.33 (s, 1H), 5.18 (t, *J* = 9.3 Hz, 1H), 5.11 – 5.06 (m, 1H), 4.94 (dd, *J* = 10.5, 3.5 Hz, 1H), 4.90 – 4.85 (m, 1H), 4.79 (dd, *J* = 10.3, 3.7 Hz, 1H), 4.46 (q, *J* = 9.3, 8.1 Hz, 3H), 4.16 – 4.04 (m, 3H), 3.93 – 3.83 (m, 2H), 3.78 (d, *J* = 9.7 Hz, 1H), 3.63 – 3.54 (m, 2H), 3.48 – 3.40 (m, 1H), 3.36 – 3.31 (m, 1H), 2.13 (s, 3H), 2.11 (d, *J* = 6.2 Hz, 3H), 2.04 (d, *J* = 9.8 Hz, 12H), 1.95 (s, 3H).

Synthesis of Compound 11: To a solution of Compound 10 Bis (2-picoly) amine (BPA) (502 mg, 2.52 mmol) in THF (12 mL) was added propargyl bromide (2.52 mL, 2.52 mmol) followed by addition of K₂CO₃ (1.04 g, 7.56 mmol). The mixture was stirred at room temperature until the starting material had completely disappeared as judged by TLC. After removing the solvent under reduced pressure, the residue was purified by column chromatography (CH₂Cl₂/MeOH=40:1) to give compound 11 as yellow oil, yield 95.34%.

¹H NMR (400 MHz, Chloroform-*d*) δ 8.08 (d, *J* = 4.8 Hz, 2H), 7.16 (td, *J* = 7.6, 1.7 Hz, 2H), 7.06 (d, *J* = 7.8 Hz, 2H), 6.69-6.63 (m, 2H), 3.48 (s, 4H), 2.98 (s, 2H), 1.98 (s, 1H).

Synthesis of Compound 12: Dissolve compound 11 (50 mg, 0.21 mmol), Compound 9 (151.6 mg, 0.21 mmol) in 1.5 mL of BuOH to obtain a reaction system solution. Mix TBTA (44.6 mg, 0.084 mmol) with CuSO₄ (20.9 mg, 0.084 mmol) solution, disperse with ultrasound, add NaVc (33.3 mg, 0.168 mmol), add reaction system solution to the mixed system, and then add H₂O to it to make V_{H₂O}/V_{BuOH}=1:1. With ultrasound assistance, the reaction stops after 10 hours at room temperature. Separation by silica gel column chromatography with Hex: EA=1:1 to get compound 12, yield 65.4 %.

¹H NMR (600 MHz, Chloroform-*d*) δ 8.54 (s, 2H), 7.67 (t, *J* = 7.0 Hz, 3H), 7.60 (d, *J* = 6.2 Hz, 2H), 7.17 (s, 2H), 5.33 (d,

$J = 3.4$ Hz, 1H), 5.19 (t, $J = 9.3$ Hz, 1H), 5.12 – 5.07 (m, 1H), 4.94 (dd, $J = 10.3, 3.4$ Hz, 1H), 4.92 – 4.88 (m, 1H), 4.51 – 4.44 (m, 3H), 4.43 – 4.34 (m, 2H), 4.15 – 4.11 (m, 1H), 4.09 – 4.03 (m, 2H), 3.96 – 3.81 (m, 8H), 3.78 (t, $J = 9.5$ Hz, 1H), 3.58 (ddd, $J = 9.7, 5.0, 1.9$ Hz, 1H), 3.44 (ddd, $J = 9.8, 8.0, 4.5$ Hz, 1H), 2.14 (s, 4H), 2.10 (s, 1H), 2.08 (s, 2H), 2.05 (t, $J = 5.0$ Hz, 1H), 2.02 (s, 2H), 1.95 (s, 3H).

HRMS (ESI): m/z calcd for $[C_{44}H_{57}N_6O_{18}]$:957.3723; Found:957.3728.

Synthesis of **Compound 13**: To a 25mL eggplant shaped bottle, compound 12 (50 mg, 0.0522mmol) in dry MeOH (8 mL) was added and 1 M NaOMe in MeOH was slowly added dropwise at room temperature. The resulting mixture was stirred for 1 hour at room temperature. The reaction pH was then adjusted with Amberlite IR-120 plus (H^+) to pH 6 and the solvent was removed under reduced pressure, yield 78.1%.

1H NMR (600 MHz, DMSO- d_6) δ 8.46 - 8.43 (m, 2H), 8.07 (s, 1H), 7.73 (td, $J = 7.7, 1.7$ Hz, 2H), 7.54 (d, $J = 7.8$ Hz, 2H), 7.23 – 7.19 (m, 2H), 4.66 (s, 1H), 4.59 (d, $J = 3.7$ Hz, 1H), 4.51 (s, 1H), 4.42 (t, $J = 6.8$ Hz, 2H), 4.16 (dt, $J = 7.0, 3.1$ Hz, 2H), 4.07 (s, 8H), 3.61 – 3.54 (m, 3H), 3.52 – 3.44 (m, 3H), 3.42 (d, $J = 5.9$ Hz, 1H), 3.37 – 3.20 (m, 8H), 3.05 – 2.99 (m, 1H).

^{13}C NMR (150 MHz, DMSO- D_6) δ 159.50, 149.29, 143.72, 137.16, 124.72, 124.64, 123.11, 122.68, 104.39, 104.32, 103.17, 98.99, 81.21, 76.06, 75.39, 73.78, 72.26, 72.16, 71.27, 71.11, 68.68, 65.98, 64.32, 60.95, 59.36, 49.15, 48.77, 46.90, 46.82, 40.95, 40.93, 30.55, 30.35.

HRMS (ESI): m/z calcd for $[C_{30}H_{43}N_6O_{11}]^+$:663.2984; Found:663.2998.

Synthesis of Compound **Fe-Lac**: Dissolve 7.4 mg of $FeCl_3$ in 2 mL of methanol solution, add compound 13 (30mg, 0.045mmol), which is also dissolved in 3.5 mL of methanol, and stir for 3 h. After the reaction is completed, the solvent is removed to obtain solid **compound 12**.

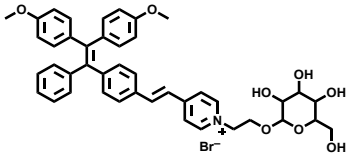
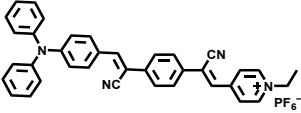
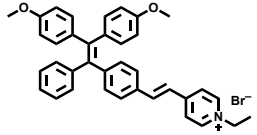
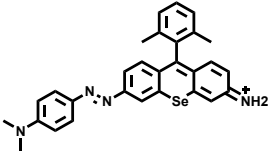
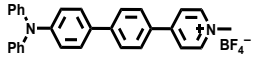
MS (ESI): m/z calcd for $[C_{30}H_{42}Cl_2FeN_6O_{11}]^+$: 788.16; Found: 788.164.

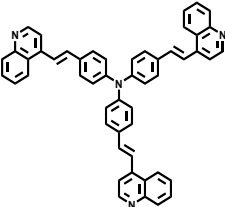
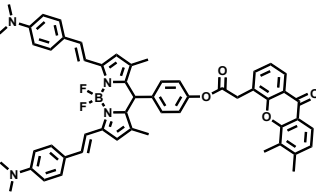
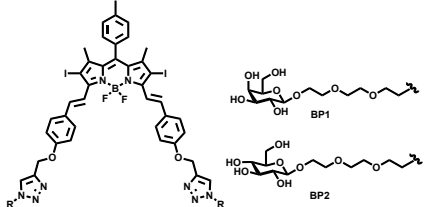
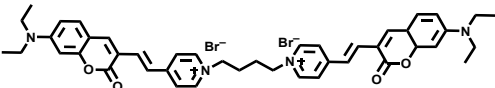
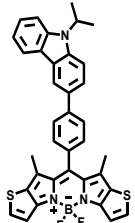
Synthesis of Compound **BT-TPE@Fe-Lac**: Dissolve **BT-TPE** (20mg, 0.037mmol) in MeOH/ CH_2Cl_2 =3:2, add 10 μ L of triethylamine (1.0 eq) for deprotonation, and then add compound 12 (60mg, 0.076mmol), heat the entire mixture under reflux at 30 ° C for 3 hours, and wash the product with cold ethanol ether to obtain the final product **BT-TPE@Fe-Lac**.

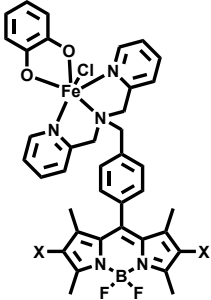
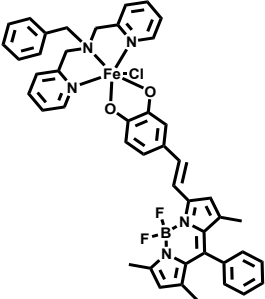
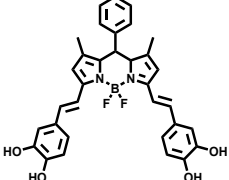
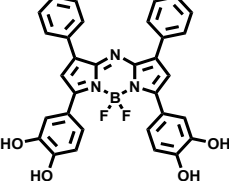
HRMS (ESI): m/z calcd for $[C_{92}H_{102}Fe_2N_{14}O_{26}S]^{2+}$:981.2749; Found:981.2753.

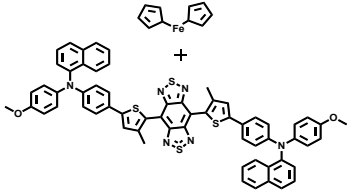
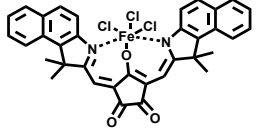
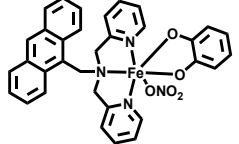
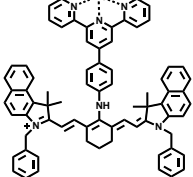
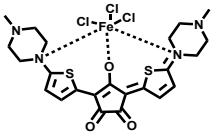
3. Supporting tables and figures

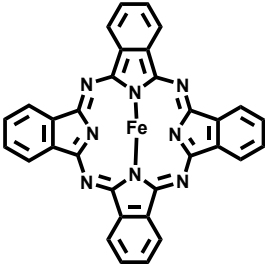
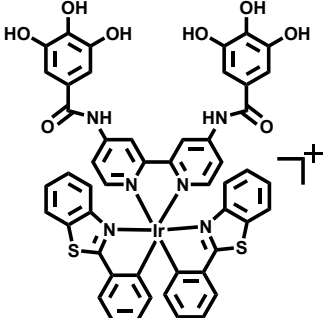
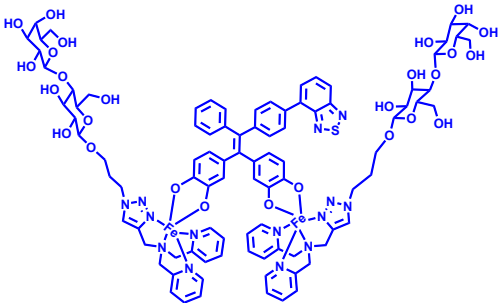
Table S1. Some reported drug used to PDT/CDT

Entry	Structure	Water solubility	Assembly method	Type of ROS	PDT/CDT	IC ₅₀	Organelle specificity	References
1		PBS	self-assembles	¹ O ₂	PDT	-	No	1
2		DMSO/water (v/v = 1/100)	self-assembles	¹ O ₂	PDT	3.98μM	Mitochondria	2
3		PBS	electrostatic-induced aggregation	¹ O ₂	PDT	-	No	3
4		PBS	self-assembles	¹ O ₂	PDT	-	No	4
5		PBS	self-assembles	¹ O ₂	PDT	-	Mitochondria	5

6		PBS	self-assembles	$^1\text{O}_2$	PDT	750 μM	Lysosome	6
7		PBS	self-assembled with mPEG-PPDA	$\text{O}_2^{\bullet-}$	PDT	2.31 and 3.90 $\mu\text{g mL}^{-1}$	No	7
8		PBS	self-assembles	$^1\text{O}_2$, $\text{O}_2^{\bullet-}$	PDT	-	No	8
9		PBS	self-assembles	$^1\text{O}_2$, $\text{O}_2^{\bullet-}$	PDT	-	cell membrane	9
10		PBS	self-assembles	$\text{O}_2^{\bullet-}$	PDT	-	Mitochondria	10

11		1% DMSO/DPBS	self-assembled	$^1\text{O}_2$,	PDT 、 CDT	6 μM /18 μM	Mitochondria	11
12		1% DMSO/DPBS	self-assembled	$^1\text{O}_2$, $\bullet\text{OH}$	PDT 、 CDT	0.08 μM	Lysosome	12
13		PBS	self-assembled with F127	$\bullet\text{OH}$	CDT	30 and 19.4 $\mu\text{g}\bullet$ mL^{-1}	No	13
14		PBS	self-assembled with F127	$\bullet\text{OH}$	CDT	-	No	14

15		PBS	self-assembled with DHA-PEG	•OH	CDT	-	No	15
16		PBS	self-assembled with BSA	•OH	CDT	-	No	16
17		1% DMSO	self-assembled	¹ O ₂ , •OH	PDT 、 CDT	6.2±0.1 μM/ 11.3±0.1 μM	nuclear DNA	17
18		PBS	self-assembled with DSPE-PEG	•OH	CDT	-	No	18
19		PBS	self-assembled with PAE-PEG- COOH	¹ O ₂ , •OH	PDT 、 CDT	20μM	No	19

20		PBS	self-assembled with DSPE-PEG	$^1\text{O}_2$ 、 $\cdot\text{OH}$	CDT	-	No	20
21		PBS	self-assembled with Fe and PEG and exosomes	$^1\text{O}_2$ 、 $\text{O}_2^{\cdot-}$ 、 $\cdot\text{OH}$	PDT、CDT	-	Lysosome	21
22	 <p data-bbox="412 1206 618 1238">BT-TPE@Fe-Lac</p>	PBS	self-assembled	$\text{O}_2^{\cdot-}$ 、 $\cdot\text{OH}$	PDT、CDT	1.2 μM	Lysosome	This work

The photophysical and photochemical properties.

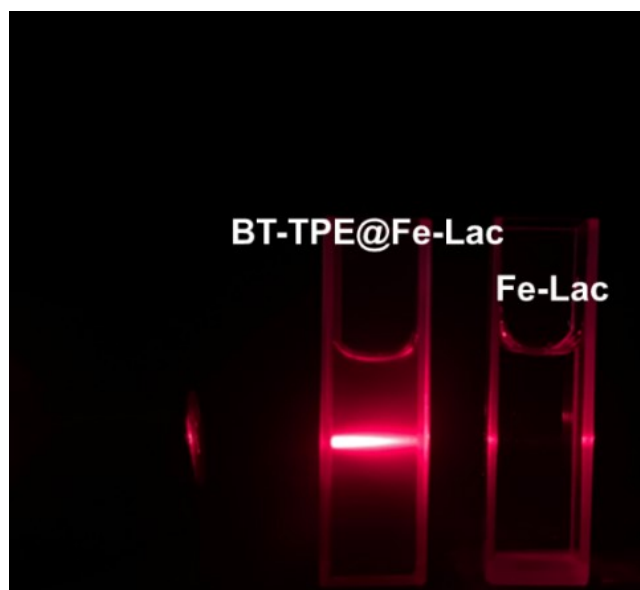


Figure S1. Tyndall effect of the aqueous solution of nano-assembly BT-TPE@Fe-Lac.

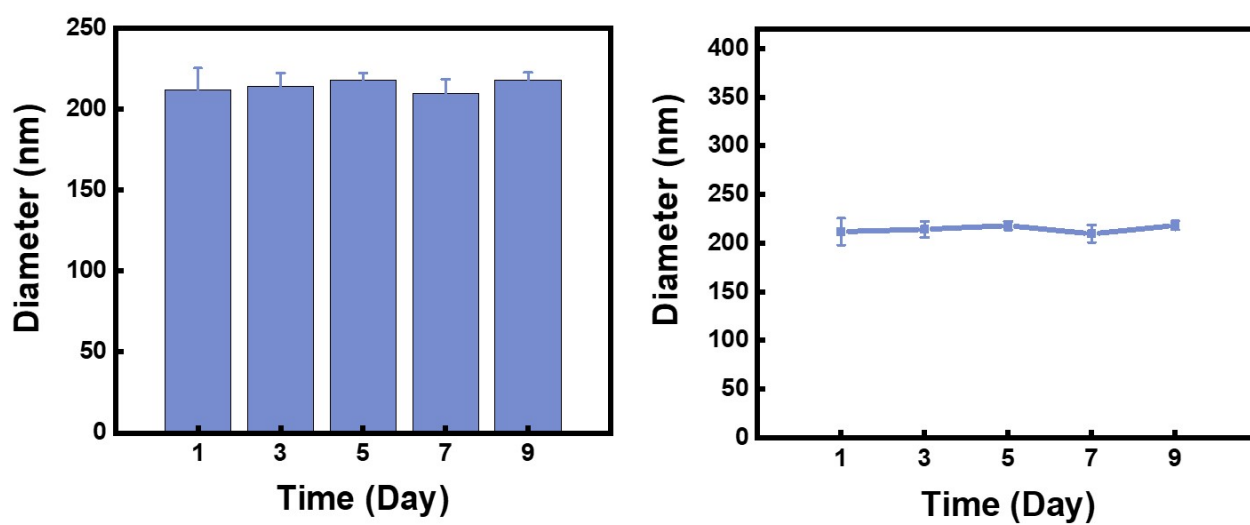


Figure S2. Stability of BT-TPE@Fe-Lac at pH 7.4.

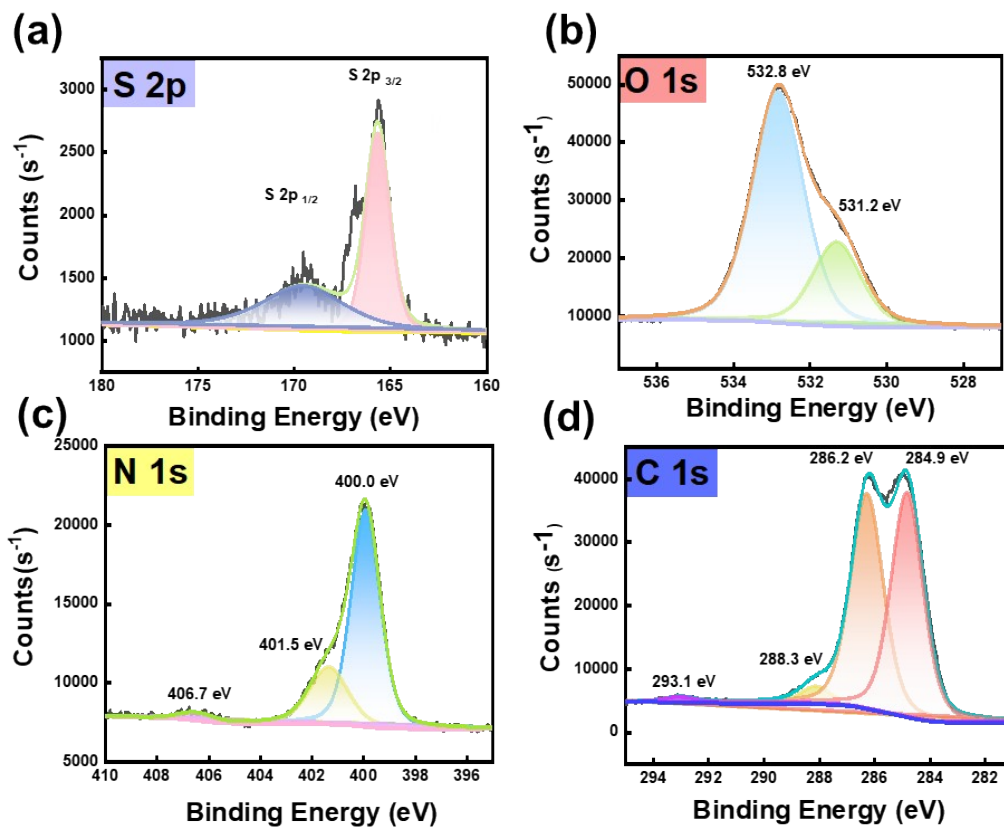


Figure S3. High-resolution X-ray photoelectron spectroscopy spectra of BT-TPE@Fe-Lac NPs. (a) S, (b) O, (c) N, (d) C.

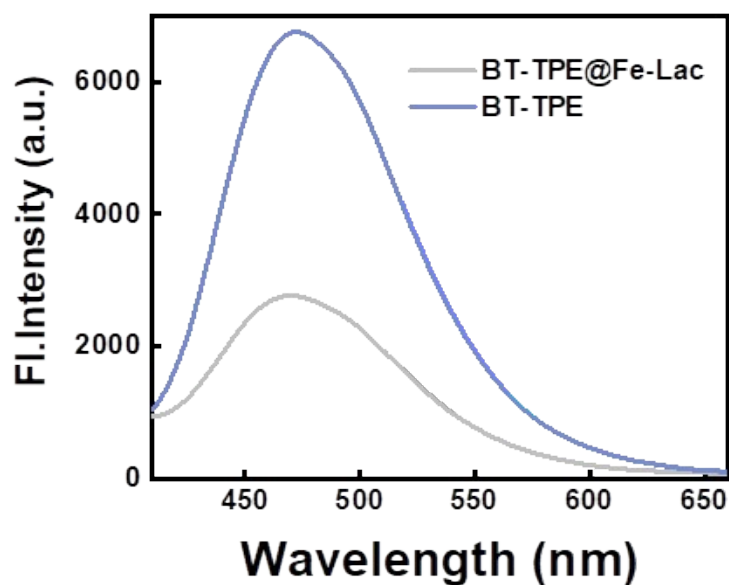


Figure S4. Emission spectra of BT-TPE (1 μM), and BT-TPE@Fe-Lac (1 μM).

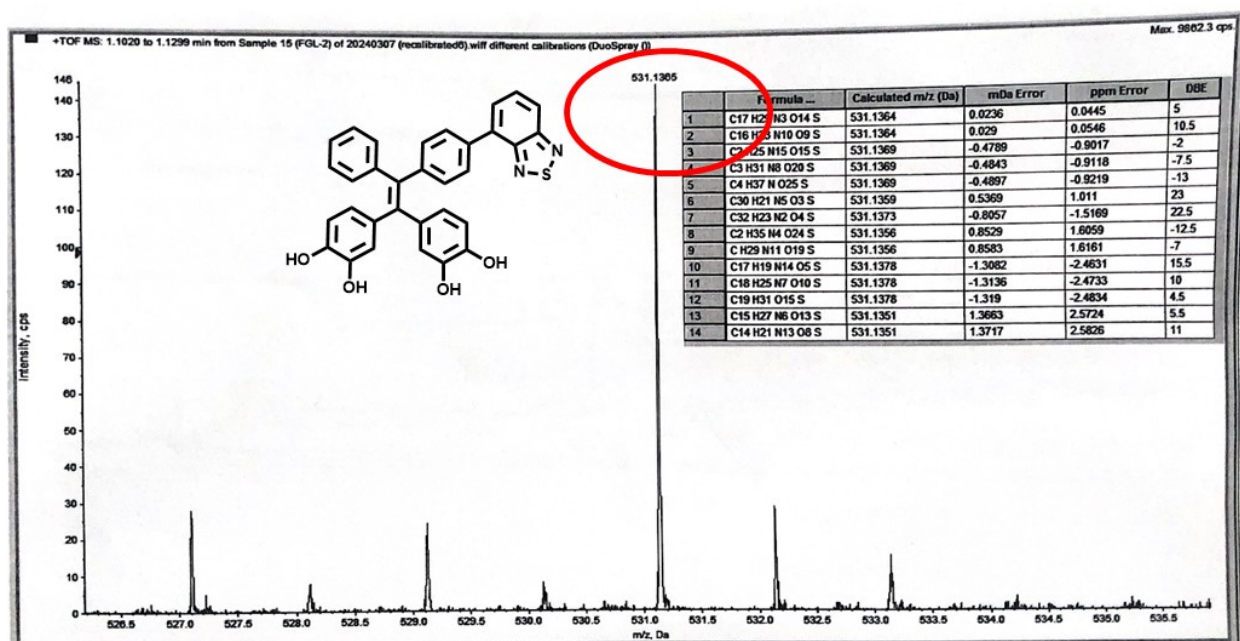


Figure S5. HRMS spectrum of compound **BT-TPE** after acid addition.

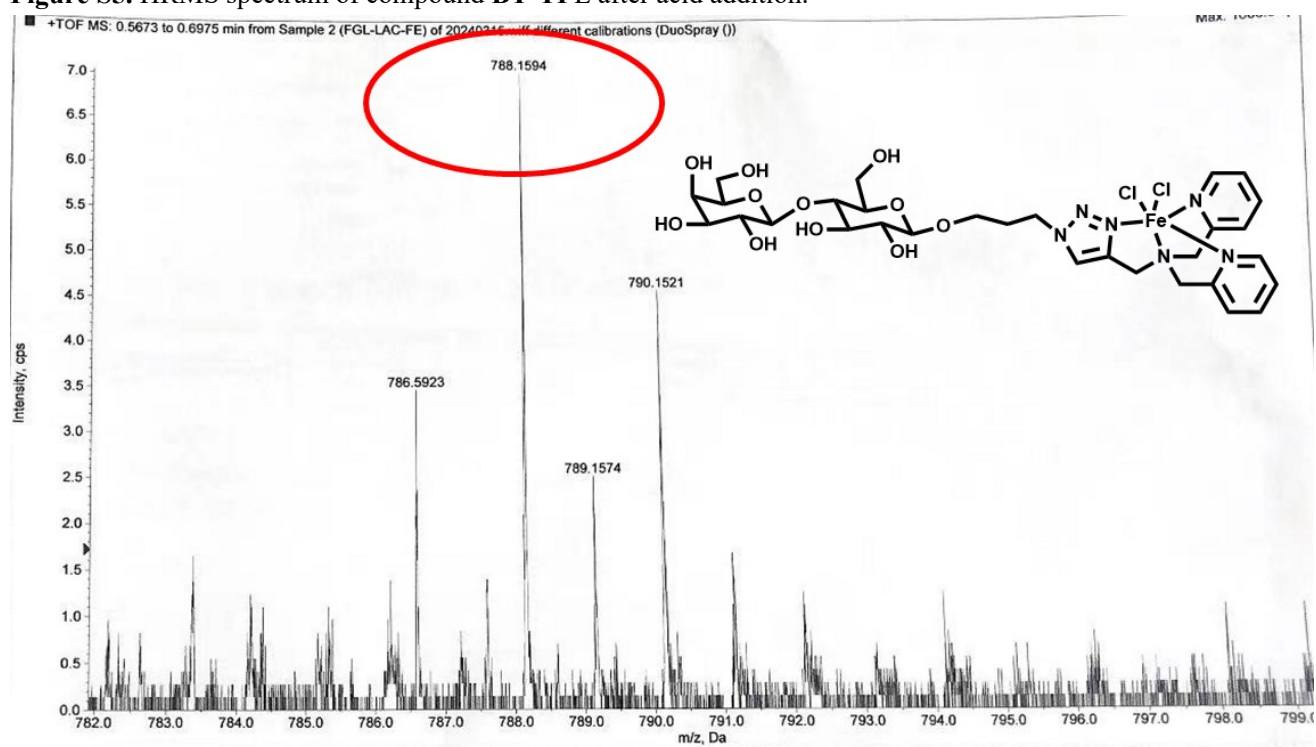


Figure S6. MS spectrum of **Fe-Lac** after acid addition.

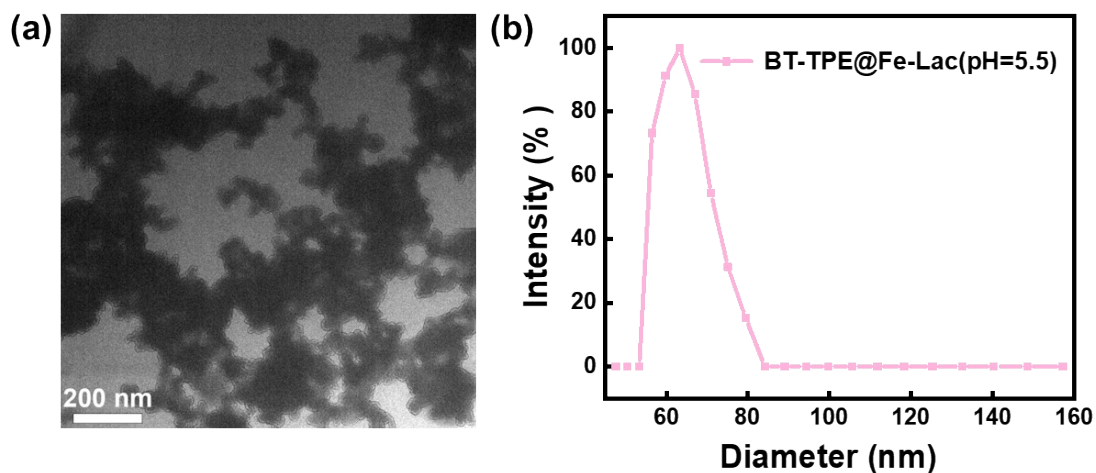


Figure S7 (a)TEM (b) DLS image of BT-TPE@Fe-Lac (1 μ M) at pH 5.4.

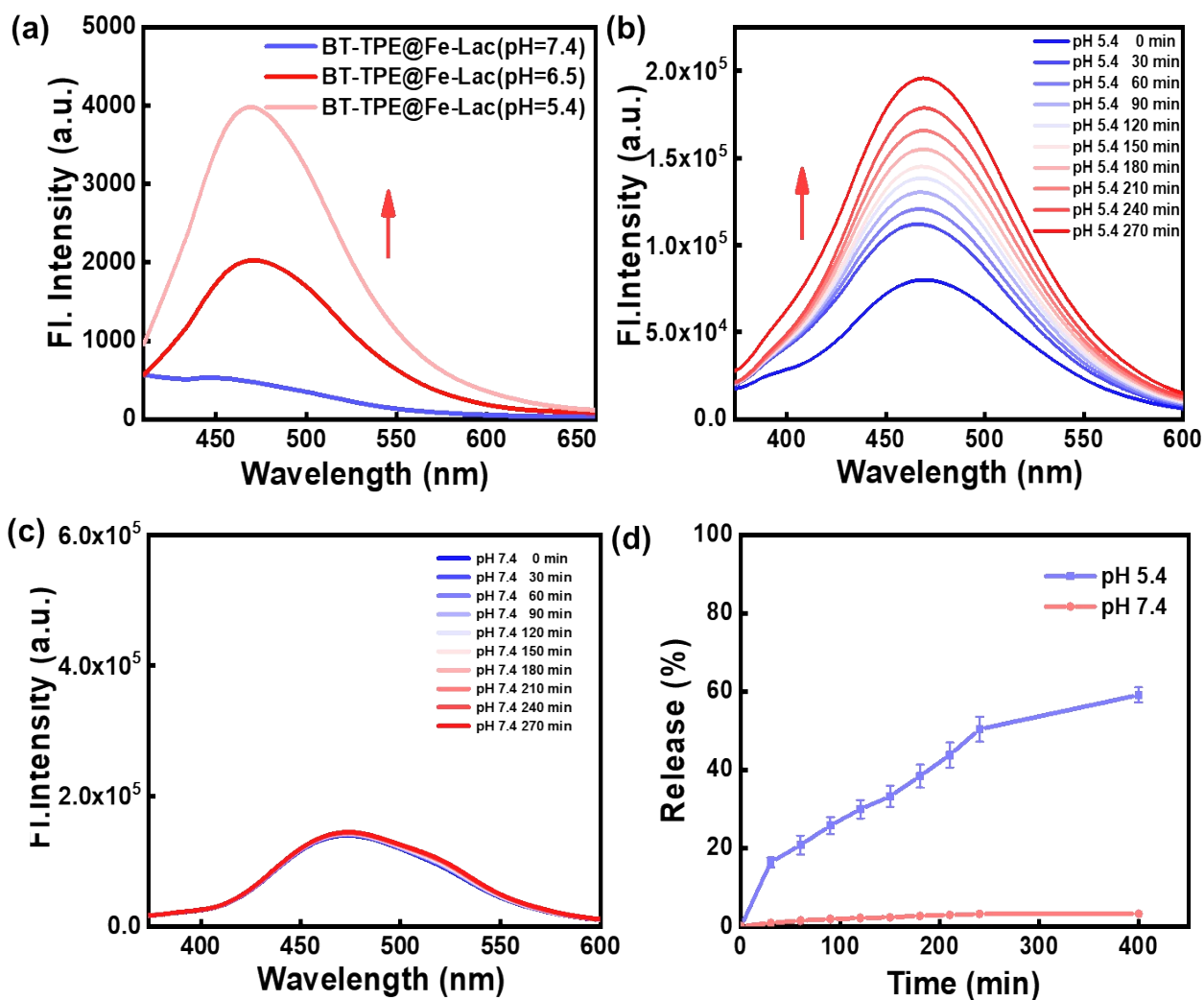


Figure S8. (a) The fluorescence intensity of BT-TPE@Fe-Lac under various pH conditions. Changes in the fluorescence intensity of BT-TPE@Fe-Lac (1 μ M) under various conditions. (b) pH 5.5, (c) pH 7.4. (d)Time-dependent release of BT-TPE from BT-TPE@Fe-Lac NPs at pH 7.4 and 5.5 .

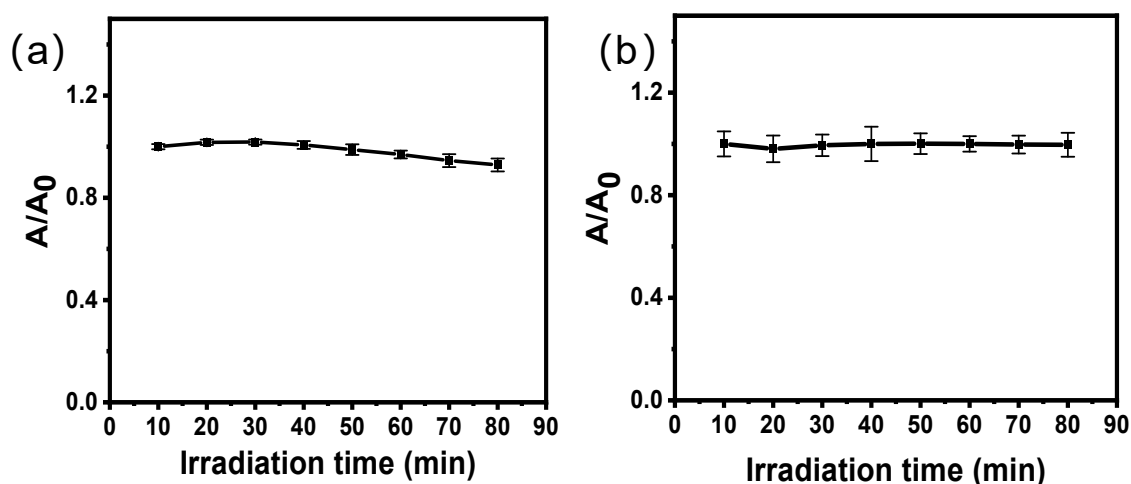


Figure S9. The A/A_0 at 312 nm of a) BT-TPE b)BT-TPE@Fe-Lac NPs in PBS at different times under the illumination of LED light (white LED light, 40 mW/cm²).

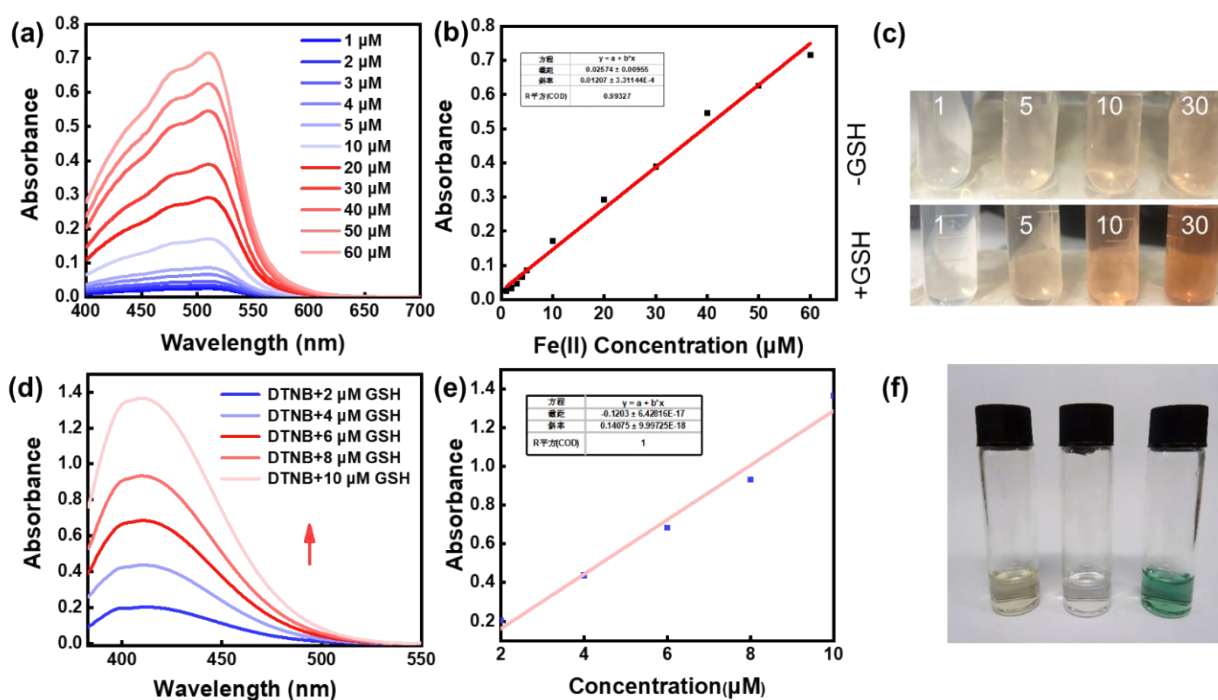


Figure S10. (a) Changes in the UV-Vis absorption spectra of Fe(II) solution at different concentrations from 1 μM to 60 μM . (b) Standard Fe(II) concentration-absorbance. (c) Changes in the UV-Vis absorption spectra at different concentrations of BT-TPE@Fe-Lac + GSH (1mM). (d) Changes in the UV-Vis absorption spectra of DTNB (1 μM) at different GSH solution concentrations from 2 μM to 10 μM . (e) Standard curve line of GSSG. (f) The color change of ABTS in different solutions, from left to right: BT-TPE@Fe-Lac+ GSH+ ABTS; GSH+ H₂O₂+ ABTS; BT-TPE@Fe-Lac+ GSH+ H₂O₂+ ABTS.

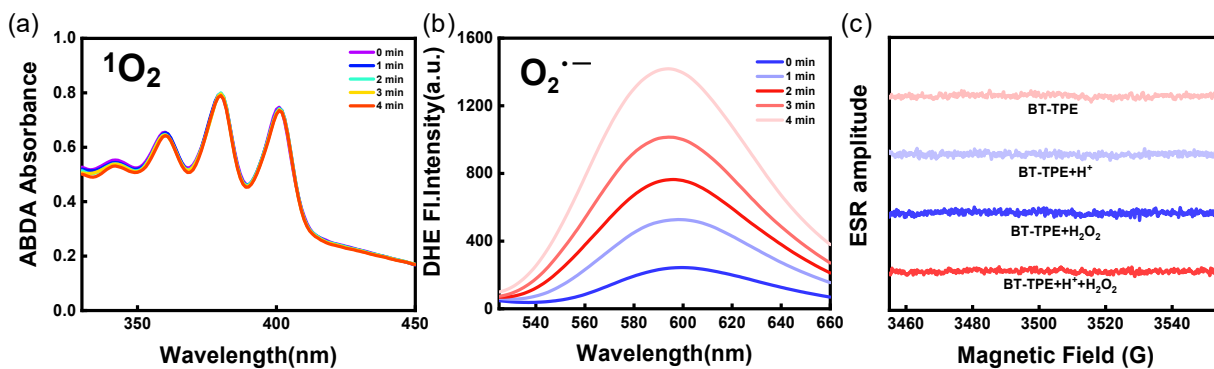


Figure S11. (a) Absorption spectra of ABDA (b) Fluorescence spectra of DHE (40 μM , excitation at 510 nm, detection from 525 to 660 nm) containing 500 $\mu\text{g/ml}$ ctDNA for different times in the presence of **BT-TPE@Fe-Lac** in PBS solution with pH 5.4. (c) Electron spin resonance spectra of **BT-TPE** upon incubation with the $\cdot\text{OH}$ scavenger 5,5-dimethyl-1-pyrroline-N-oxide in the presence of H_2O_2 and acidic conditions.

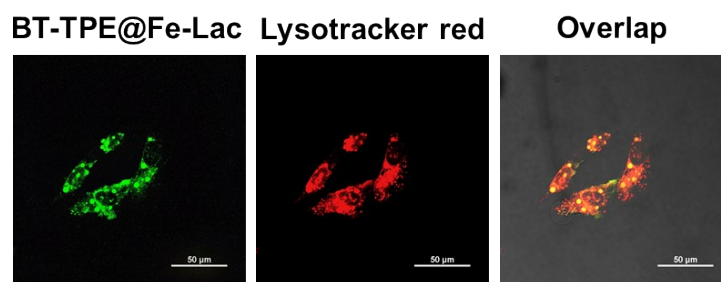


Figure S12. CLSM images of HepG2 cells incubated with **BT-TPE@Fe-Lac**, and lysotracker red. Scale bar: 50 μm .

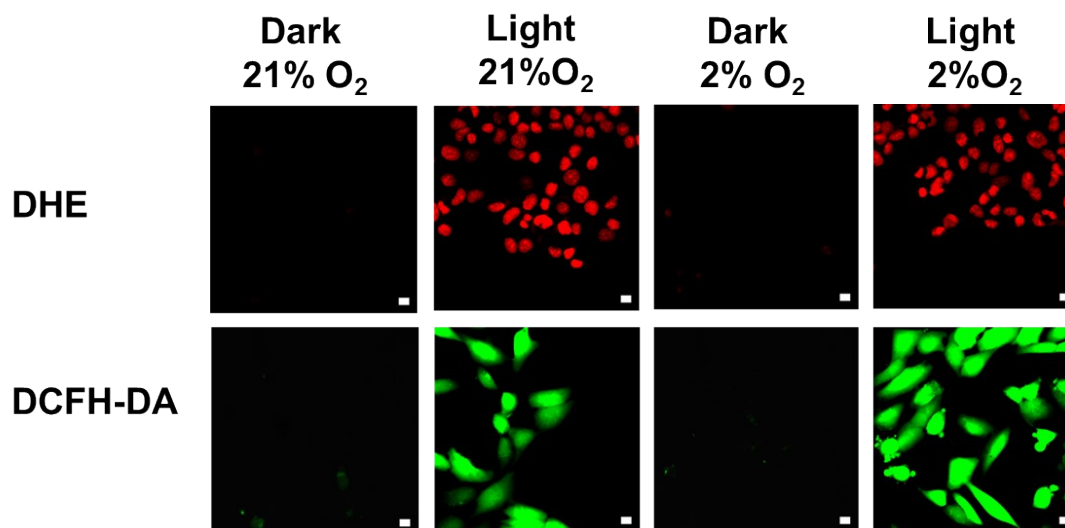


Figure S13. Detection of ROS and $\text{O}_2^{\cdot-}$ detection in HepG2 cells under normoxia (21% O_2) and hypoxia (2% O_2) conditions by using DCFH-DA and DHE. Scale bars: 10 μm .

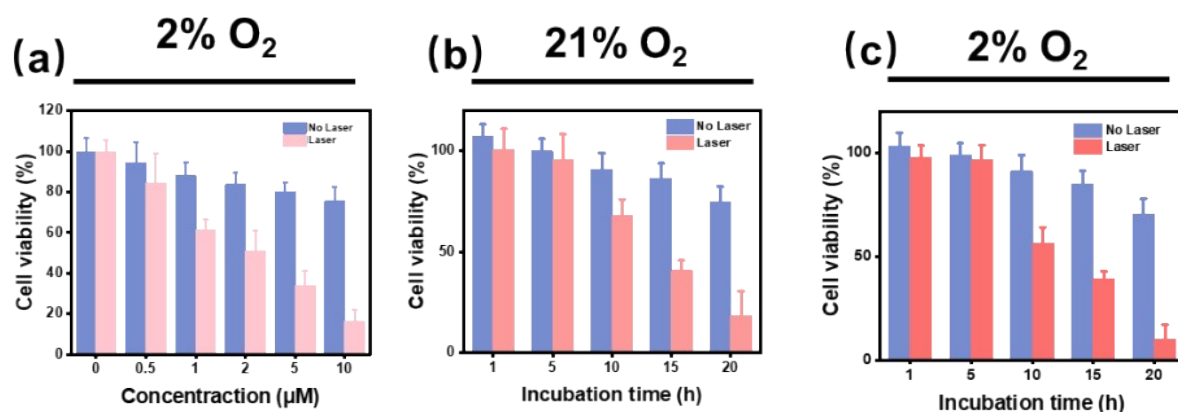


Figure S14. (a) Concentration-dependent cell viability of **BT-TPE@Fe-Lac** treated HepG2 cells in the absence or presence of light irradiation under hypoxic conditions. Time-dependent cell viability of 1.0 μM **BT-TPE@Fe-Lac** treated HepG2 cells in the absence or presence of light irradiation under (b) normoxic and (c) hypoxic conditions.

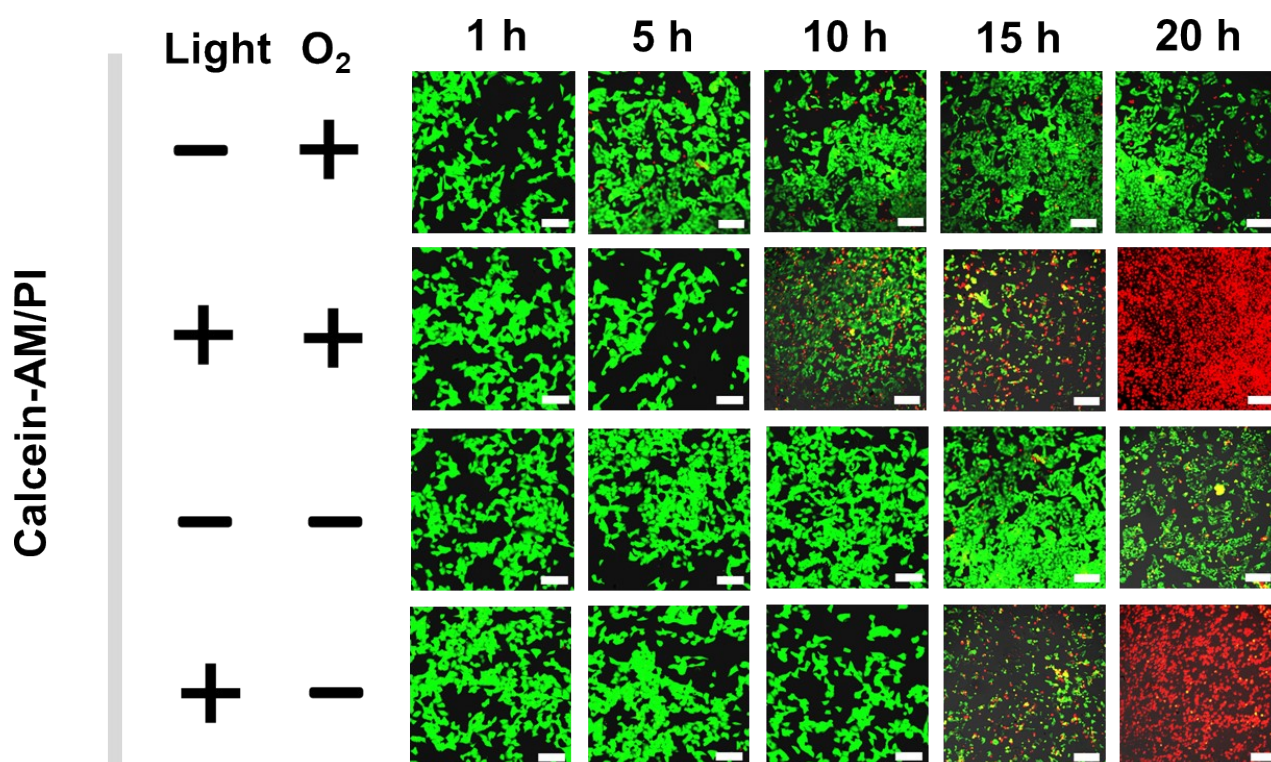


Figure S15. CLSM images of **BT-TPE@Fe-Lac**-treated HepG2 cells in the absence or presence of light irradiation under normoxic and hypoxic conditions. The live and dead cells were stained with calcein-AM and PI, respectively. Scale bars: 200 μm .

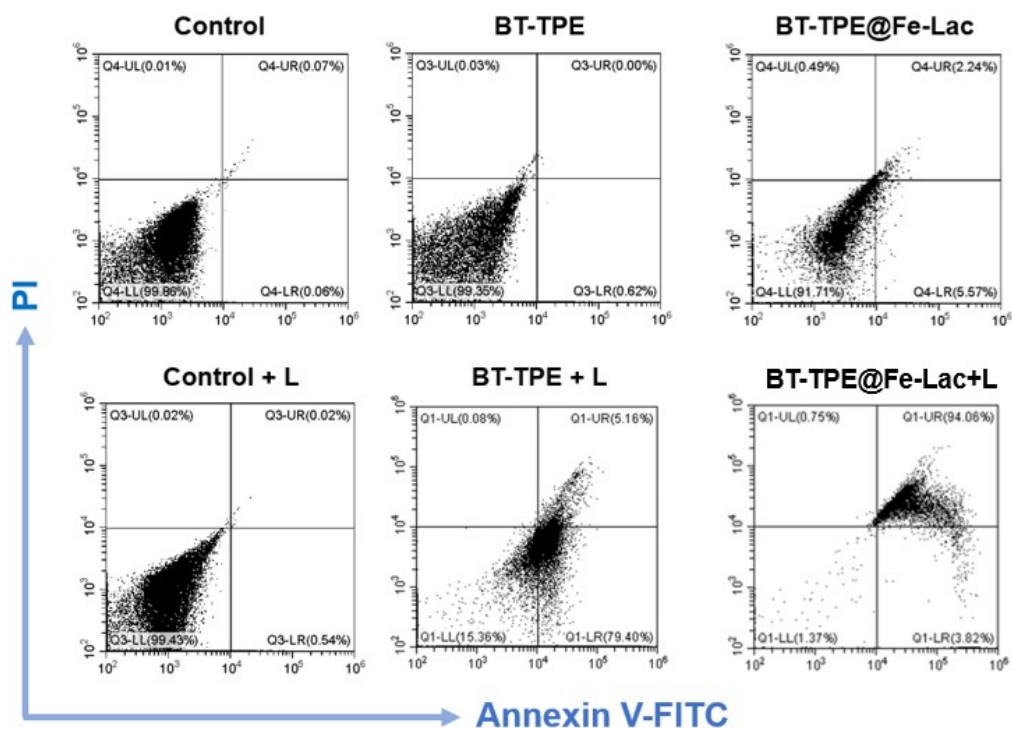


Figure S16. Flow cytometry of Annexin V/PI stained HepG2 cells treated with control, **BT-TPE** (2 μ M), and **BT-TPE@Fe-Lac** (2 μ M) with or without laser.

4. NMR spectra and MS spectra

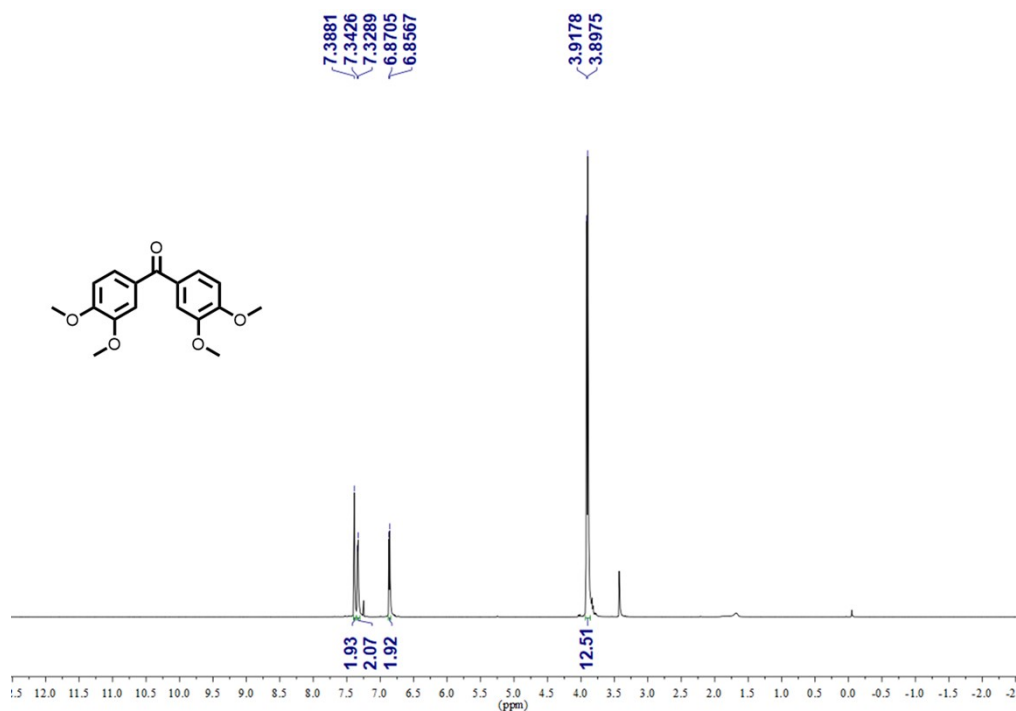


Figure S17. ¹H-NMR spectra of **compound 2** in CDCl₃.

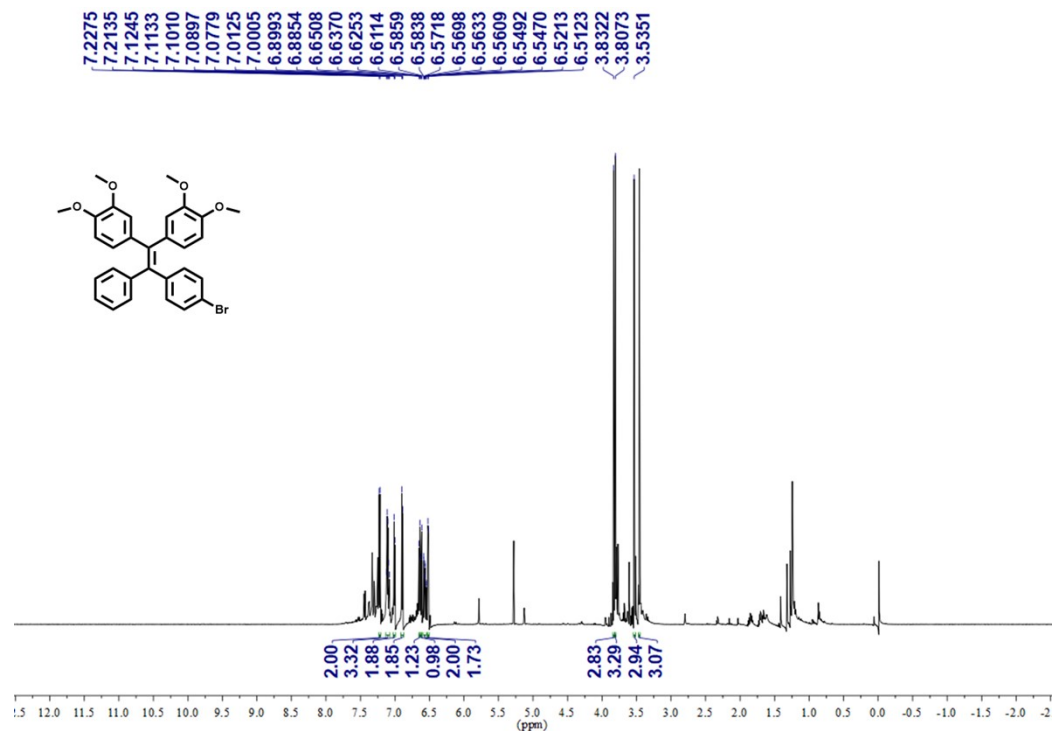


Figure S18. ¹H-NMR spectra of compound 3 in CDCl₃.

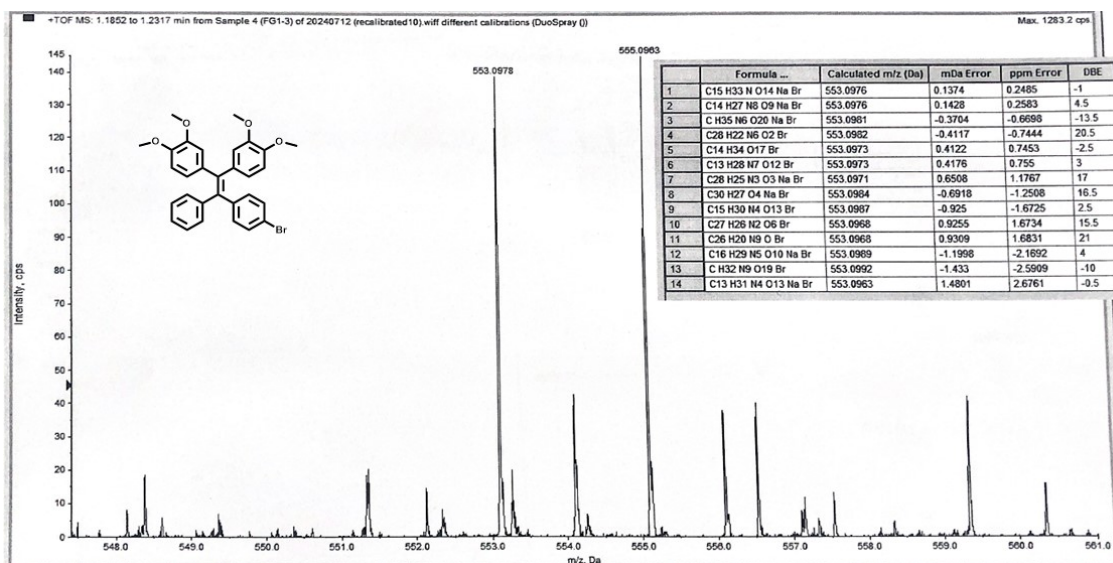


Figure S19. HRMS spectra of compound 3 in CDCl₃.

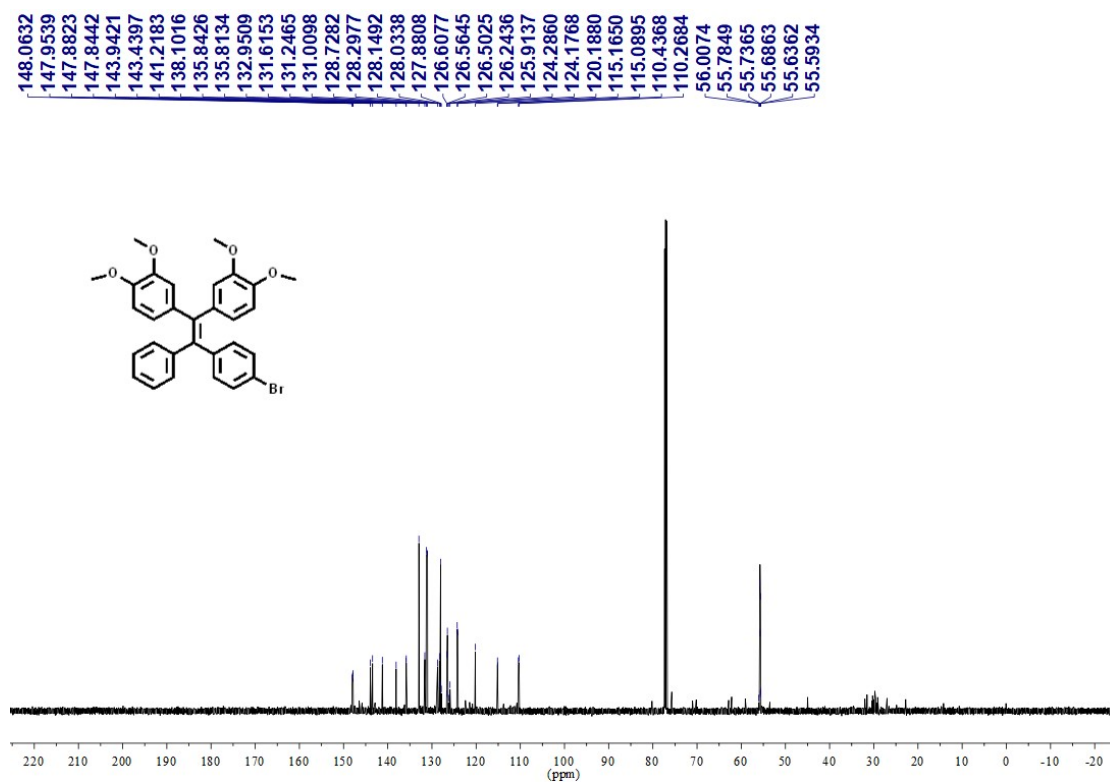


Figure S20. ¹³C-NMR spectra of compound 3 in CDCl₃.

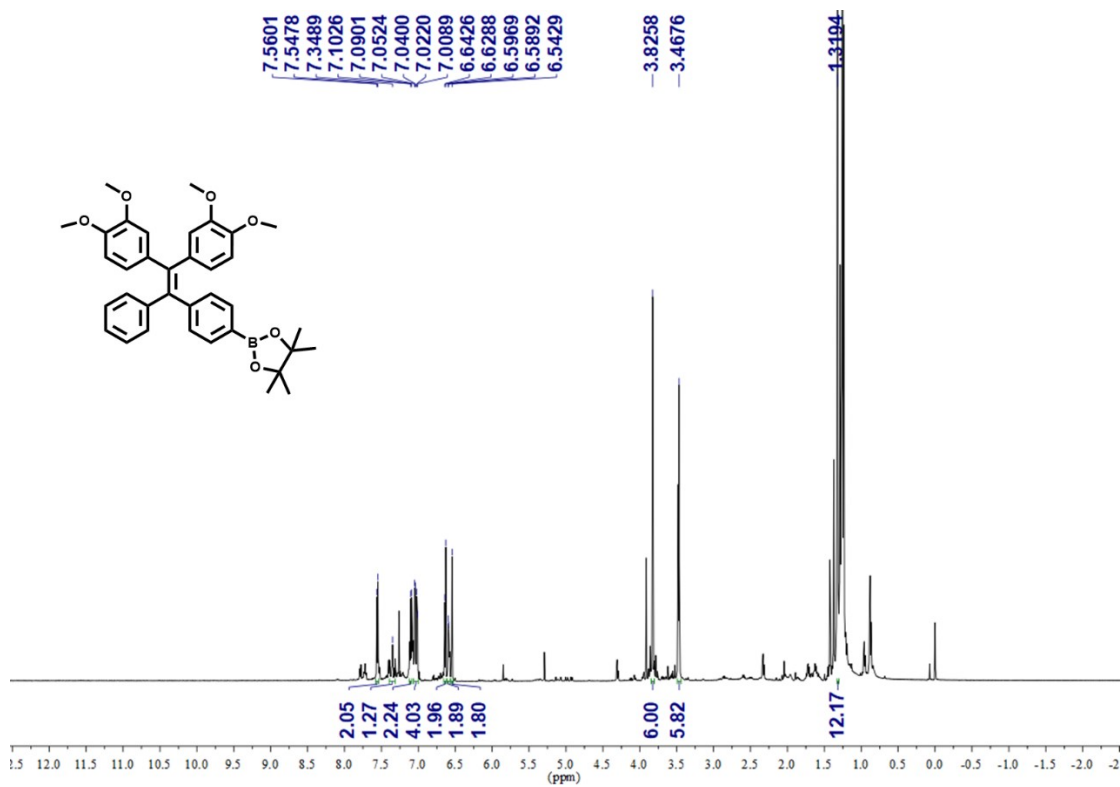


Figure S21. ¹H-NMR spectra of compound 4 in CDCl₃.

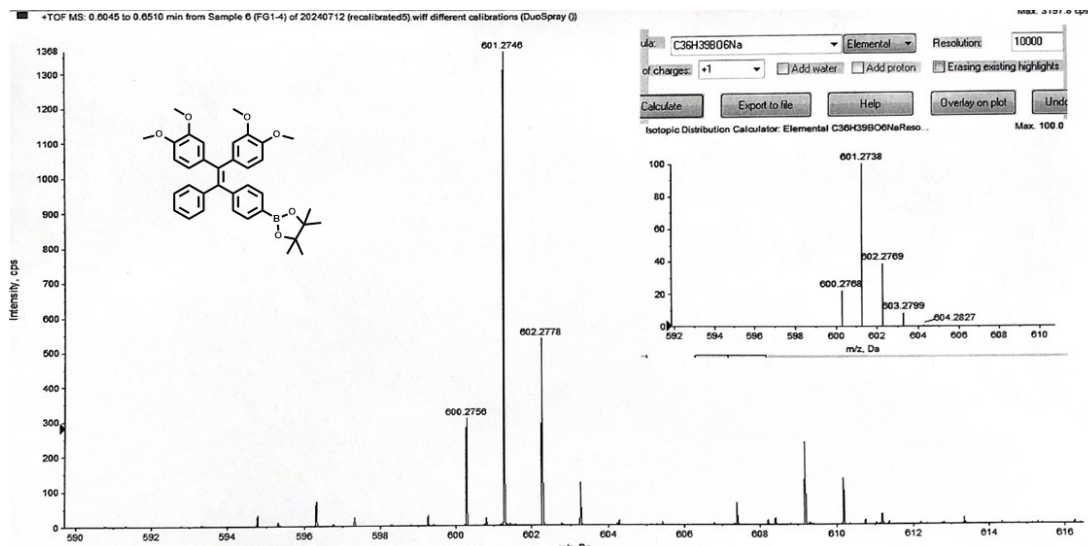


Figure S22. HRMS spectra of **compound 4** in CDCl₃.

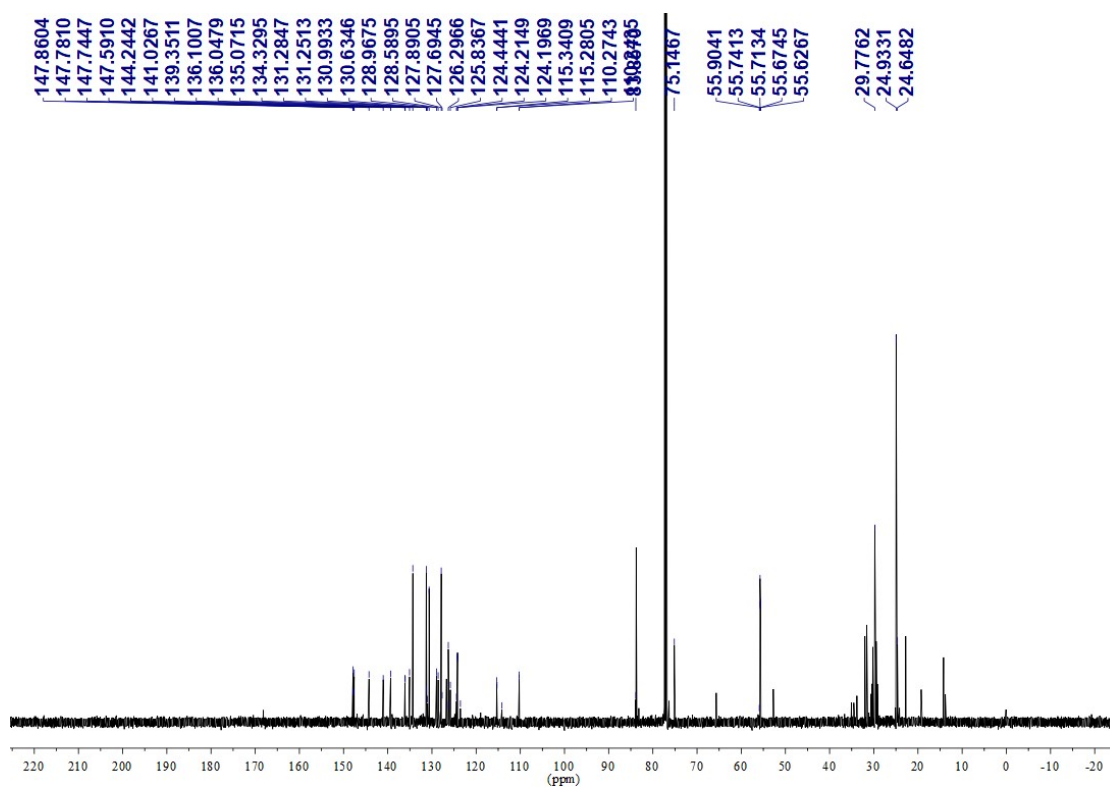


Figure S23. ¹³C-NMR spectra of **compound 4** in CDCl₃.

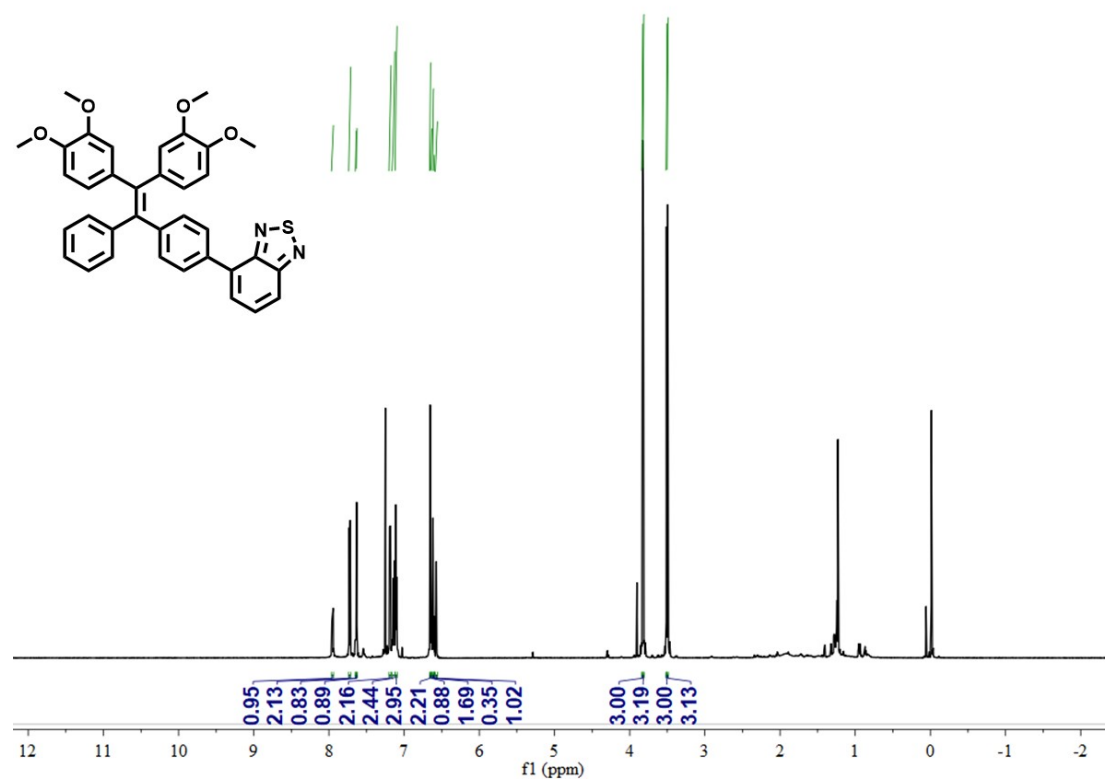


Figure S24. $^1\text{H-NMR}$ spectra of compound **5** in CDCl_3 .

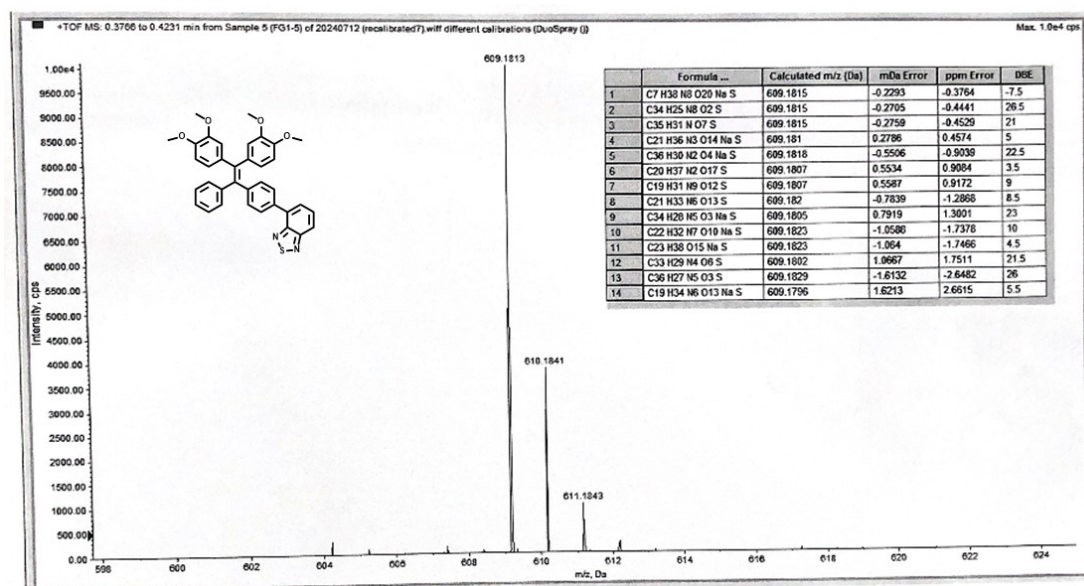


Figure S25. HRMS spectra of compound **5** in CDCl_3 .

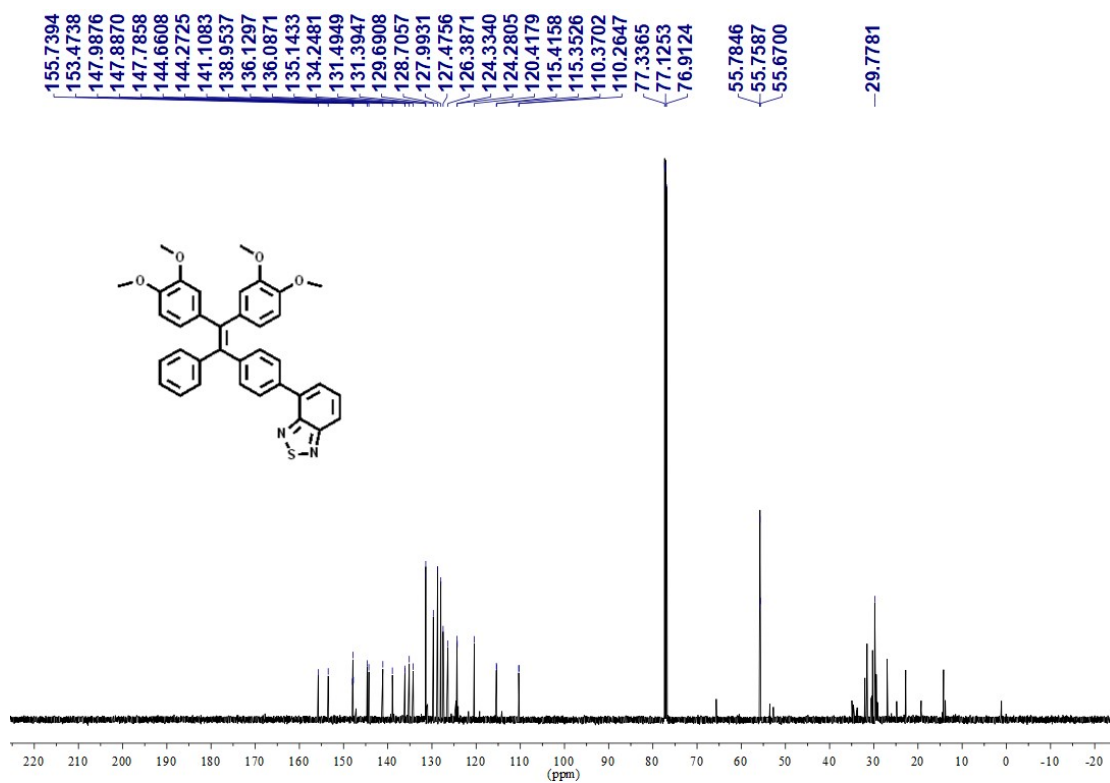


Figure S26. ¹³C-NMR spectra of compound 5 in CDCl₃.

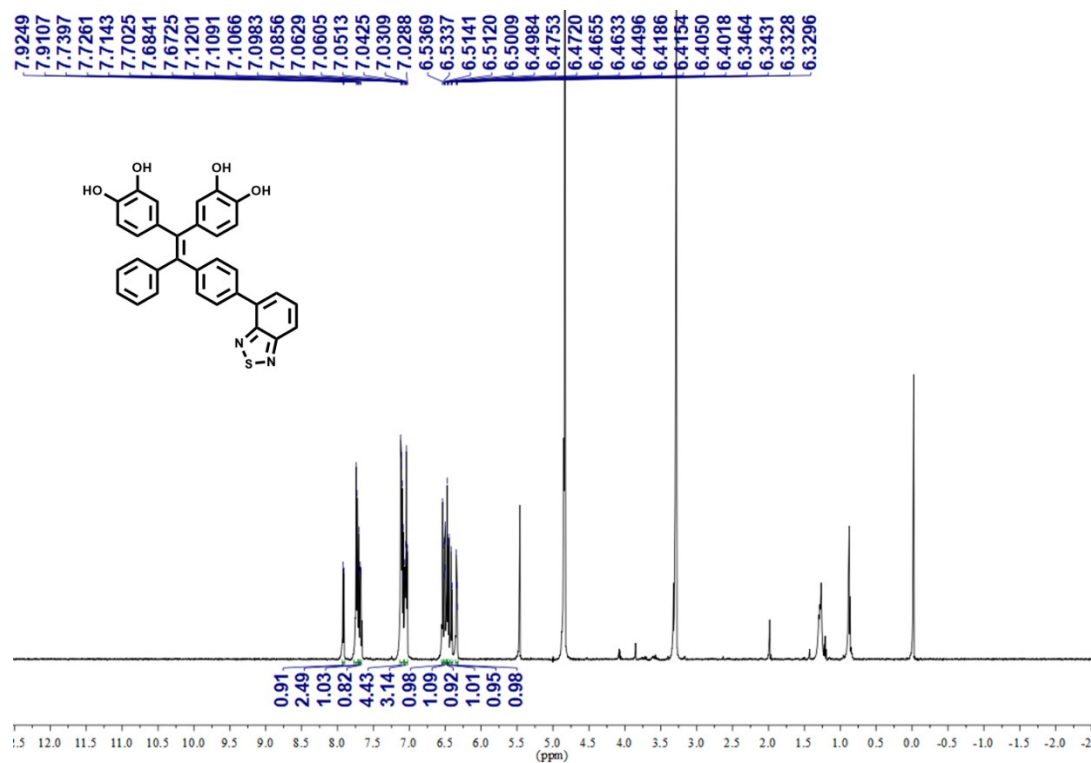


Figure S27. ¹H-NMR spectra of compound BT-TPE in CDCl₃.

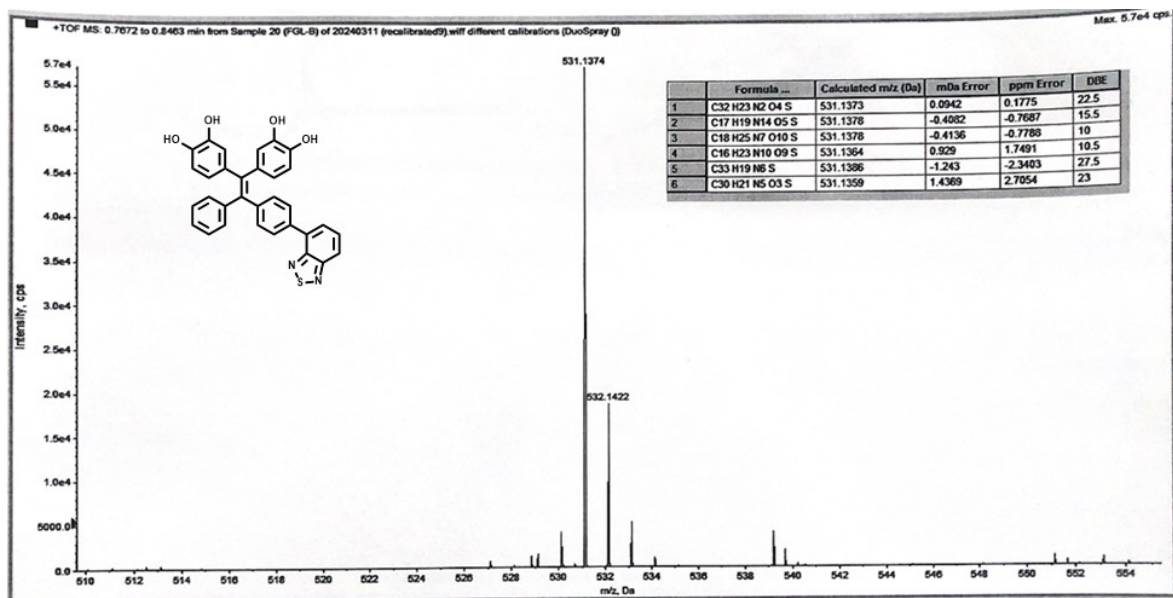


Figure S28. HRMS spectrum of compound BT-TPE.

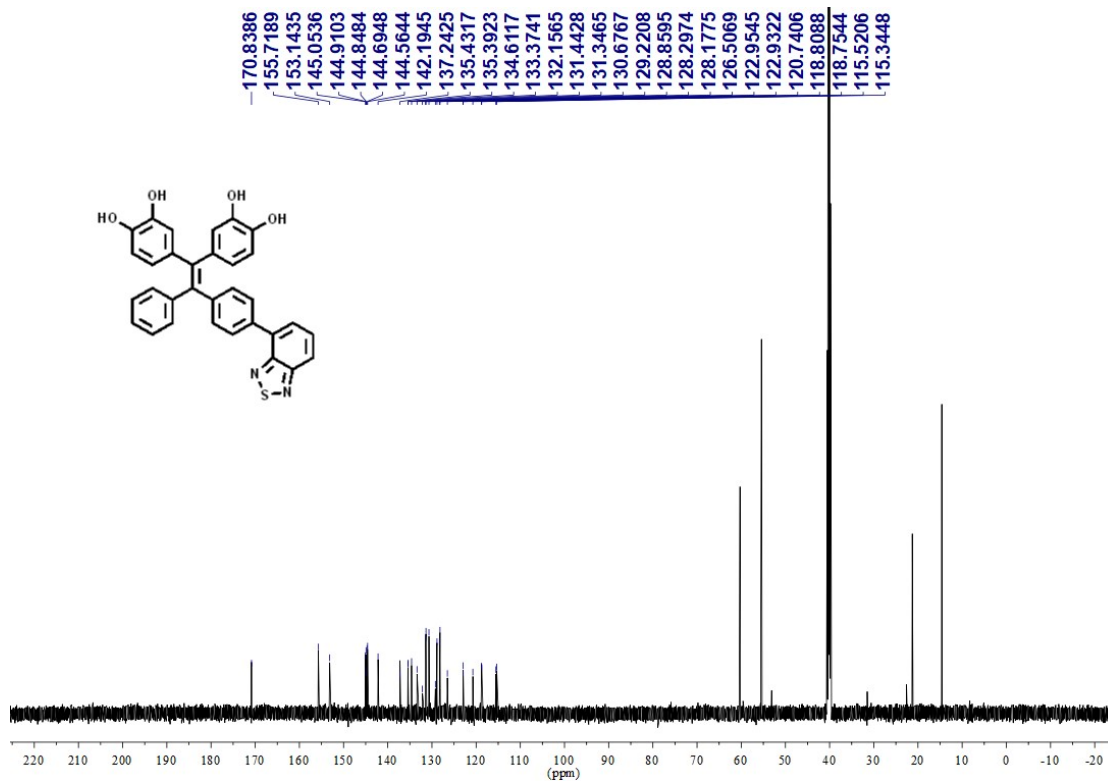


Figure S29. ^{13}C -NMR spectrum of compound BT-TPE.

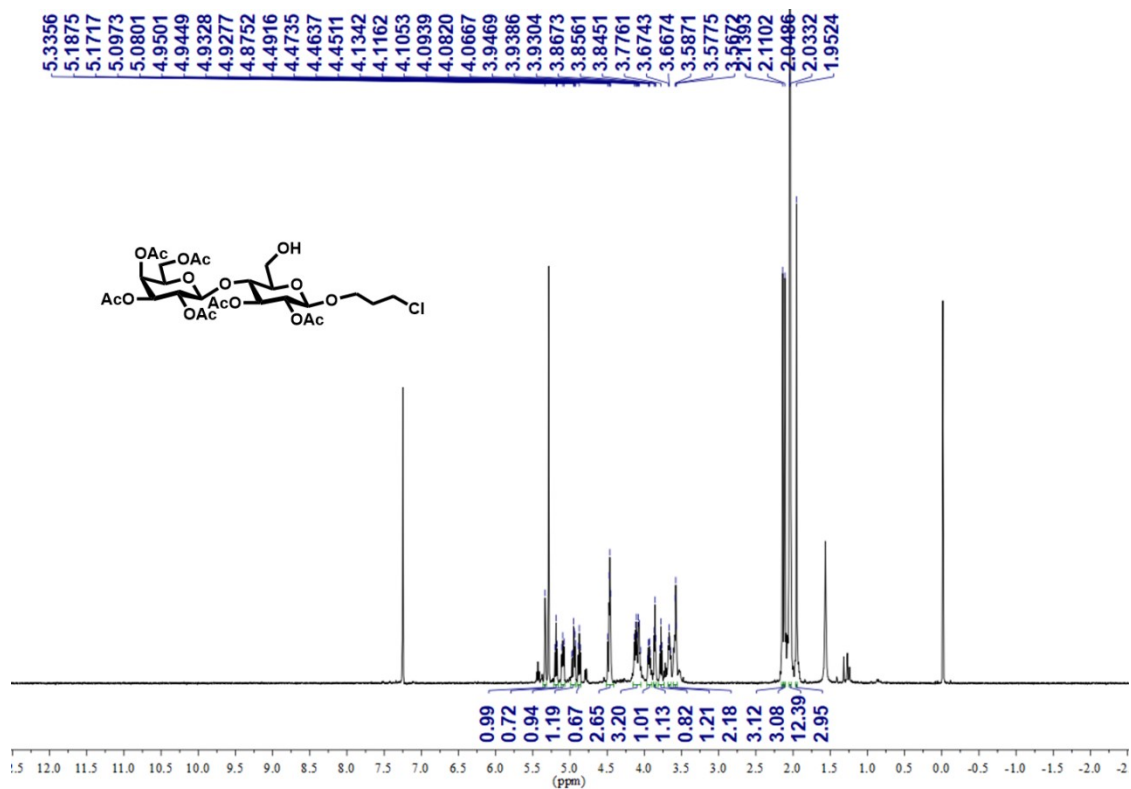


Figure S30. ¹H-NMR spectra of compound 8 in CDCl₃.

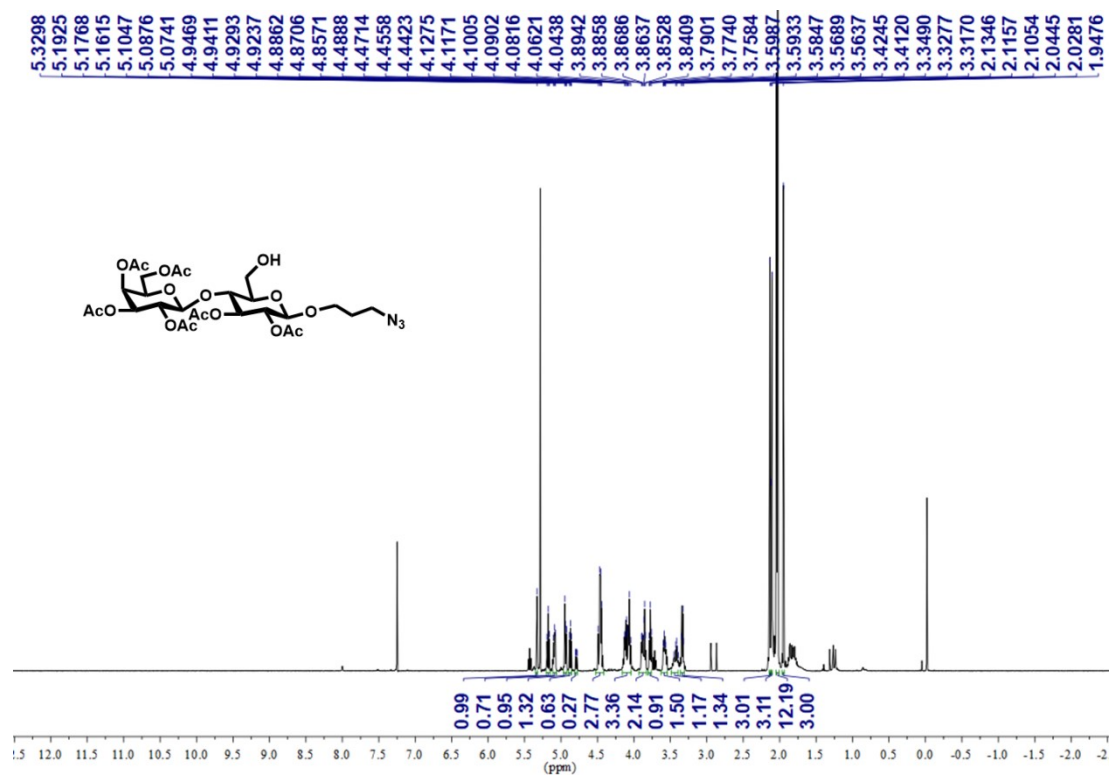


Figure S31. ¹H-NMR spectra of compound 9 in CDCl₃.

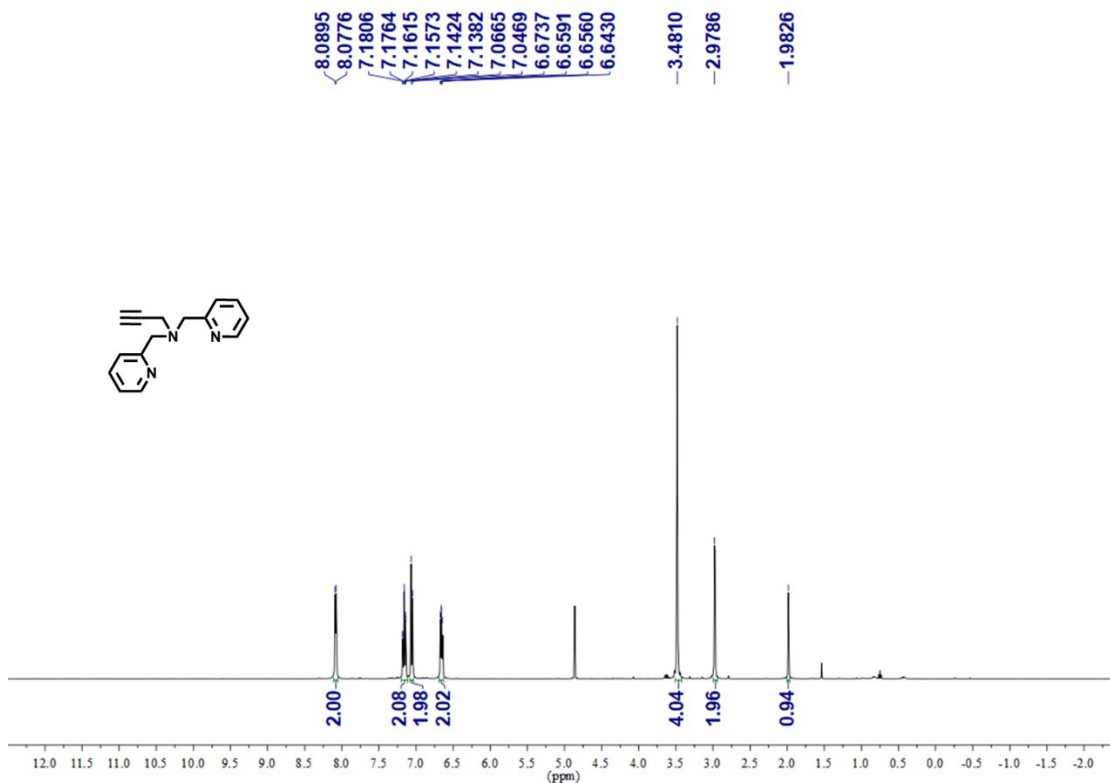


Figure S32. ¹H-NMR spectra of compound 11 in CDCl₃.

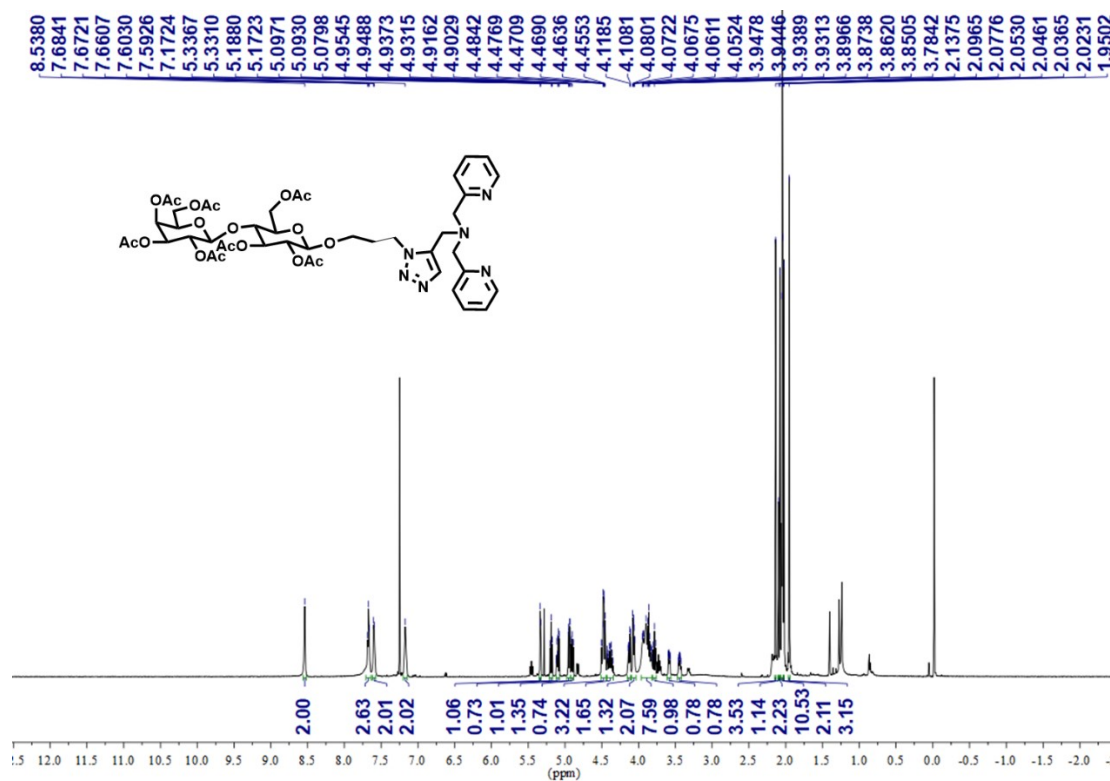


Figure S33. ¹H-NMR spectra of compound 12.

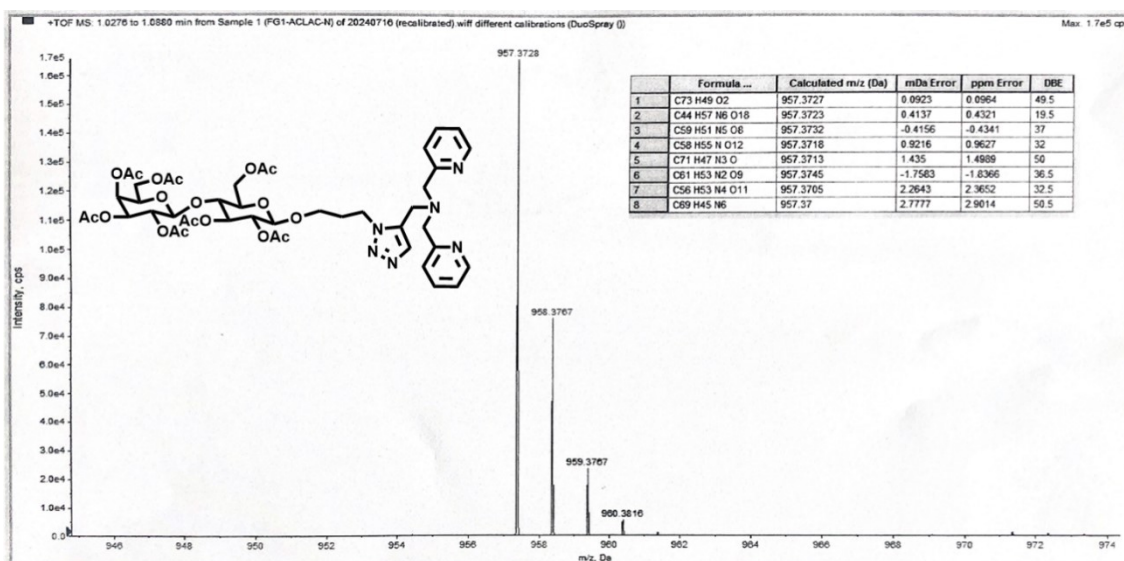


Figure S34. ¹H-NMR spectra of compound 12.

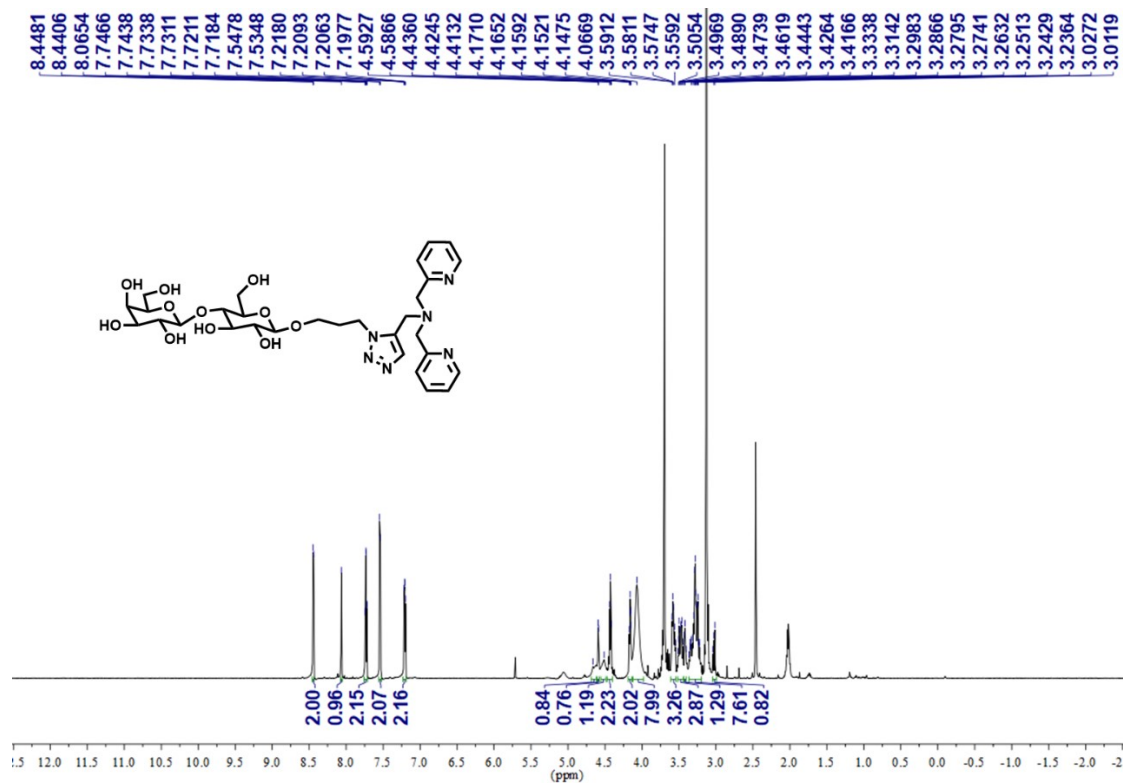


Figure S35. ¹H-NMR spectra of compound 13 in CDCl₃.

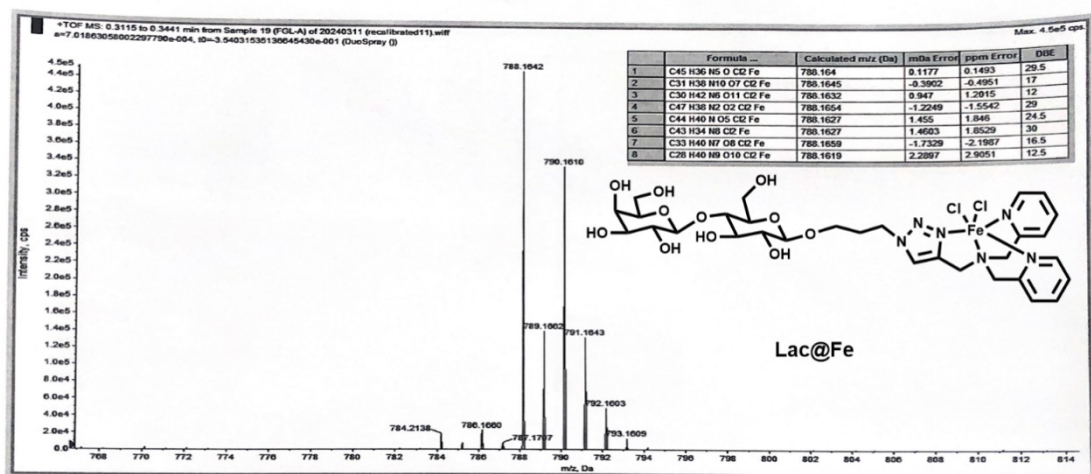


Figure S36. HRMS spectrum of compound 13.

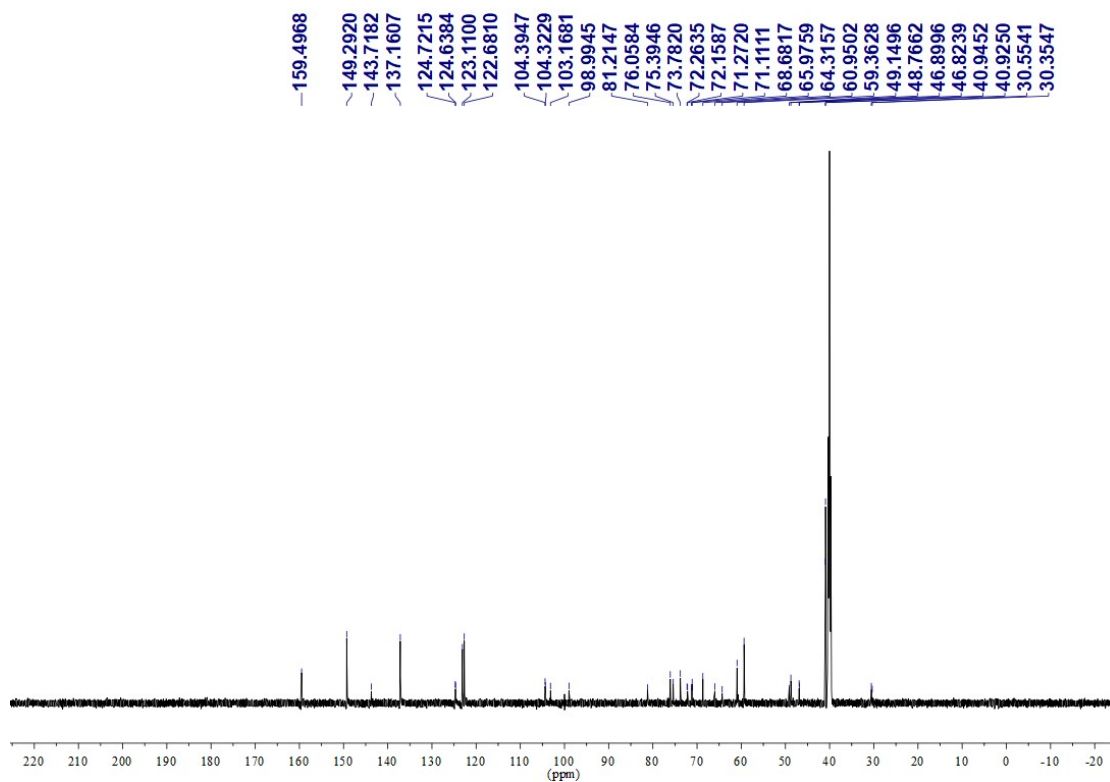


Figure S37. ¹³C-NMR spectrum of compound 13.

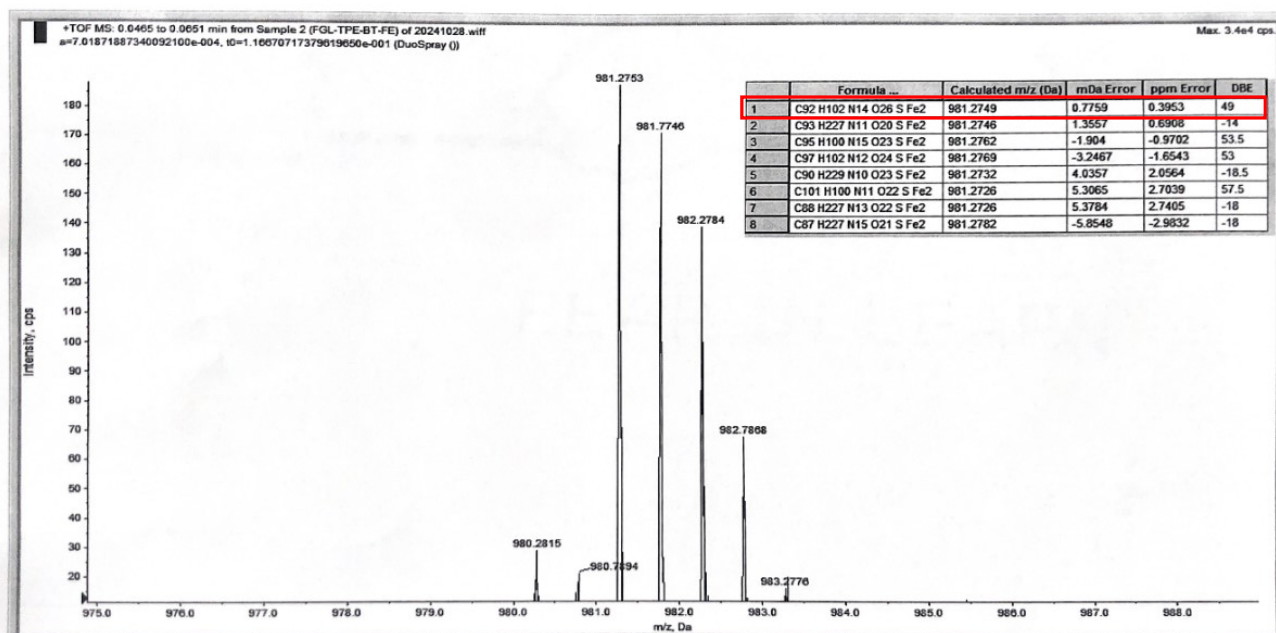


Figure S38. HRMS spectrum of BT-TPE@Fe-Lac.

5. References

- (1) Guo, Q.; Xue, S.; Feng, J.; Peng, C.; Zhou, C.; Qiao, Y., AIE - Active Glycomimetics Triggered Bacterial Agglutination and Membrane - Intercalating toward Efficient Photodynamic Antiseptic. *Adv. Health. Mater.* **2023**, 12, (26).
- (2) Zhang, S.; Yang, W.; Lu, X.; Zhang, X.; Pan, Z.; Qu, D. H.; Mei, D.; Mei, J.; Tian, H., Near-infrared AIEgens with high singlet-oxygen yields for mitochondria-specific imaging and antitumor photodynamic therapy. *Chem. Sci.* **2023**, 14, (25), 7076-7085.
- (3) Tavakkoli Yarak, M.; Pan, Y.; Hu, F.; Yu, Y.; Liu, B.; Tan, Y. N., Nanosilver-enhanced AIE photosensitizer for simultaneous bioimaging and photodynamic therapy. *Mater. Chem. Front.* **2020**, 4, (10), 3074-3085.
- (4) Piao, W.; Hanaoka, K.; Fujisawa, T.; Takeuchi, S.; Komatsu, T.; Ueno, T.; Terai, T.; Tahara, T.; Nagano, T.; Urano, Y., Development of an Azo-Based Photosensitizer Activated under Mild Hypoxia for Photodynamic Therapy. *J. Am. Chem. Soc.* **2017**, 139, (39), 13713-13719.
- (5) Zhuang, W.; Yang, L.; Ma, B.; Kong, Q.; Li, G.; Wang, Y.; Tang, B. Z., Multifunctional Two-Photon AIE Luminogens for Highly Mitochondria-Specific Bioimaging and Efficient Photodynamic Therapy. *ACS Appl. Mater. Interfaces* **2019**, 11, (23), 20715-20724.
- (6) Hu, Y.; Yin, S.; Deng, T.; Li, J., A novel pH-activated AIEgen probe for dynamic lysosome tracking and high-efficiency photodynamic therapy. *Chem. Commun.* **2024**, 6, (22), 335-347.
- (7) Chen, D.; Yu, Q.; Huang, X.; Dai, H.; Luo, T.; Shao, J.; Chen, P.; Chen, J.; Huang, W.; Dong, X., A Highly - Efficient Type I Photosensitizer with Robust Vascular - Disruption Activity for Hypoxic - and - Metastatic Tumor Specific Photodynamic Therapy. *Small* **2020**, 16, (23).
- (8) Liu, J. Y.; Tian, Y.; Dong, L., Galactosyl BODIPY-based nanoparticles as a type-I photosensitizer for HepG2 cell targeted photodynamic therapy. *RSC Adv.* **2024**, 14, (13), 8735-8739.
- (9) Bu, Y.; Xu, T.; Zhu, X.; Zhang, J.; Wang, L.; Yu, Z.; Yu, J.; Wang, A.; Tian, Y.; Zhou, H.; Xie, Y., A NIR-I light-responsive superoxide radical generator with cancer cell membrane targeting ability for enhanced imaging-guided photodynamic therapy. *Chem. Sci.* **2020**, 11, (37), 10279-10286.
- (10) Pham, T. C.; Cho, M.; Nguyen, V.; Nguyen, V. K. T.; Kim, G.; Lee, S.; Dehaen, W.; Yoon, J.; Lee, S., Charge Transfer-Promoted Excited State of a Heavy-Atom-Free Photosensitizer for Efficient Application of Mitochondria-Targeted Fluorescence Imaging and Hypoxia Photodynamic Therapy. *ACS Appl. Mater. Interfaces* **2024**, 16, (17), 21699-21708.
- (11) Garai, A.; Gandhi, A.; Ramu, V.; Raza, M. K.; Kondaiah, P.; Chakravarty, A. R., Photochemotherapy of Infrared Active BODIPY-Appended Iron(III) Catecholates for in Vivo Tumor Growth Inhibition. *ACS Omega* **2018**, 3, (8), 9333-9338.
- (12) Sahoo, S.; Pathak, S.; Kumar, A.; Nandi, D.; Chakravarty, A. R., Lysosome directed red light photodynamic therapy using glycosylated iron-(III) conjugates of boron-dipyrromethene. *J. Inorg. Biochem.* **2023**, 244, 112226.
- (13) Ou, C.; Zhang, Y.; Ge, W.; Zhong, L.; Huang, Y.; Si, W.; Wang, W.; Zhao, Y.; Dong, X., A three-dimensional BODIPY - iron(iii) compound with improved H₂O₂ -response for NIR-II photoacoustic imaging guided chemodynamic/photothermal therapy. *Chem. Commun.* **2020**, 56, (46), 6281-6284.
- (14) Zhang, J.; Li, Y.; Jiang, M.; Qiu, H.; Li, Y.; Gu, M.; Yin, S., Self-Assembled Aza-BODIPY and Iron(III) Nanoparticles for Photothermal-Enhanced Chemodynamic Therapy in the NIR-II Window. *ACS Biomater. Sci. Eng.* **2023**, 9, (2), 821-830.
- (15) Wang, Z.; Wang, Y.; Gao, H.; Tang, C.; Feng, Z.; Lin, L.; Che, S.; Luo, C.; Ding, D.; Zheng, D.; Yu, Z.; Peng, Z., Phototheranostic nanoparticles with aggregation-induced emission as a four-modal imaging platform for image-guided photothermal therapy and ferroptosis of tumor cells. *Biomaterials* **2022**, 289, 121779.
- (16) Zeng, F.; Tang, L.; Zhang, Q.; Shi, C.; Huang, Z.; Nijjati, S.; Chen, X.; Zhou, Z., Coordinating the Mechanisms of Action of Ferroptosis and the Photothermal Effect for Cancer Theranostics. *Angew. Chem. Int. Ed.* **2022**, 61, (13).
- (17) Basu, U.; Khan, I.; Hussain, A.; Kondaiah, P.; Chakravarty, A. R., Photodynamic Effect in Near - IR Light by a Photocytotoxic Iron(III) Cellular Imaging Agent. *Angew. Chem. Int. Ed.* **2012**, 51, (11), 2658-2661.
- (18) He, T.; Yuan, Y.; Jiang, C.; Blum, N. T.; He, J.; Huang, P.; Lin, J., Light - Triggered Transformable Ferrous Ion Delivery System for Photothermal Primed Chemodynamic Therapy. *Angew. Chem. Int. Ed.* **2021**, 60, (11), 6047-6054.

- (19) Sun, R.; Ma, W.; Ling, M.; Tang, C.; Zhong, M.; Dai, J.; Zhu, M.; Cai, X.; Li, G.; Xu, Q.; Tang, L.; Yu, Z.; Peng, Z., pH-activated nanoplatform for visualized photodynamic and ferroptosis synergistic therapy of tumors. *J. Control. Release* **2022**, 350, 525-537.
- (20) Gong, Y.; Wang, X.; Gong, F.; Li, G.; Yang, Y.; Hou, L.; Zhang, Q.; Liu, Z.; Cheng, L., Phthalocyanine iron nanodots for combined chemodynamic-sonodynamic cancer therapy. *Science China materials* **2022**, 65, (9), 2600-2608.
- (21) Feng, T.; Tang, Z.; Karges, J.; Shen, J.; Jin, C.; Chen, Y.; Pan, Y.; He, Y.; Ji, L.; Chao, H., Exosome camouflaged coordination-assembled Iridium (III) photosensitizers for apoptosis-autophagy-ferroptosis induced combination therapy against melanoma. *Biomaterials* **2023**, 301, 122212.